Hindawi Publishing Corporation
EURASIP Journal on Image and Video Processing
Volume 2007, Article ID 60539, 27 pages
doi:10.1155/2007/60539

Review Article

An Overview on Wavelets in Source Coding, Communications, and Networks

James E. Fowler[1] and Béatrice Pesquet-Popescu[2]

[1] *Department of Electrical & Computer Engineering, GeoResources Institute, Mississippi State University, P.O. Box 9627, Mississippi State, MS 39762, USA*
[2] *Département Traitement du Signal et des Images, École Nationale Supérieure des Télécommunications, 46 rue Barrault, 75634 Paris, France*

Received 7 January 2007; Accepted 11 April 2007

Recommended by Jean-Luc Dugelay

The use of wavelets in the broad areas of source coding, communications, and networks is surveyed. Specifically, the impact of wavelets and wavelet theory in image coding, video coding, image interpolation, image-adaptive lifting transforms, multiple-description coding, and joint source-channel coding is overviewed. Recent contributions in these areas arising in subsequent papers of the present special issue are described.

1. INTRODUCTION

Wavelet transforms are arguably the most powerful, and most widely-used, tool to arise in the field of signal processing in the last several decades. Their inherent capacity for multiresolution representation akin to the operation of the human visual system motivated a quick adoption and widespread use of wavelets in image-processing applications. Indeed, wavelet-based algorithms have dominated image compression for over a decade, and wavelet-based source coding is now emerging in other domains. For example, recent wavelet-based video coders exploit wavelet-based temporal filtering in conjunction with motion compensation to yield effective video compression with full temporal, spatial, and fidelity scalability. Additionally, wavelets are increasingly used in the source coding of remote-sensing, satellite, and other geospatial imagery. Furthermore, wavelets are starting to be deployed beyond the source-coding realm with increased interest in robust communication of images and video over both wired and wireless networks. In particular, wavelets have been recently proposed for joint source-channel coding and multiple-description coding. This special issue collects a number of papers that explore these and other latest advances in the theory and application of wavelets.

Here, in this introductory paper to the special issue, we provide a general overview of the application of wavelets and wavelet theory to the signal representation, source coding, communication, and network transmission of images and video. The main body of this paper is partitioned into two major parts: we first cover wavelets in signal representation and source coding, and then explore wavelets in communications and networking. Specifically, in Section 2, we focus on wavelets in image coding, video coding, and image interpolation, as well as image-adaptive lifting transforms. Then, in Section 3, we explore the use of wavelets in multiple-description coding and joint source-channel coding as employed in communication and networking applications. Finally, we make some concluding remarks in Section 4. Brief overviews of the papers in the special issue are presented at the end of relevant sections throughout this introductory paper—these overviews are demarked by boldfaced headings to facilitate their location.

2. WAVELETS IN SIGNAL REPRESENTATION AND SOURCE CODING

In the most elemental sense, wavelets provide an expansion set (usually a basis) that decomposes an image simultaneously in terms of frequency and space. Thus, *signal representation*—the representation of a signal using an expansion set and corresponding expansion coefficients—can perhaps be considered the most fundamental task to which wavelets are

applied. Combining such a signal representation with quantization and some form of bitstream generation yields image/video compression schemes; such *source coding* constitutes perhaps the most widespread practical application of wavelets. In this section, we overview the role of wavelets in current applications of both signal representation and source coding. First, we focus on source coding by examining the use of wavelets in image and video coders in Sections 2.1 and 2.2, respectively. In Section 2.3, we discuss image-adaptive wavelet transforms that have been proposed to improve signal-representation capabilities by adapting to local image features. Finally, in Section 2.4, we explore wavelet-based signal representations for the interpolation (magnification) of image data.

2.1. Image coding

Over the last decade, wavelets have established a dominant presence in the task of 2D image compression, and they are increasingly being considered for the compression of 3D imagery as well. Wavelets are attractive in the image-coding problem due to a tradition of excellent rate-distortion performance coupled with an inherent capacity for *progressive transmission* wherein successive reconstructions of the image are possible as more and more of the compressed bitstream is received and decoded. Below, we overview several salient concepts in the field of image coding, including multidimensional wavelet transforms, coding procedures applied to such transforms, as well as coding methodology for general imagery of shape other than traditional rectangular scenes (i.e., shape-adaptive coding). The reader is referred elsewhere for more comprehensive and in-depth surveys of 2D image coding (e.g., [1]), 3D image coding (e.g., [2]), and shape-adaptive coding (e.g., [3]).

2.1.1. Multidimensional wavelet transforms

A single stage of a 1D discrete wavelet transform (DWT) decomposes a 1D signal into a lowpass signal and a highpass signal. Multidimensional wavelet decompositions are typically constructed by such 1D wavelet decompositions applied independently along each dimension of the image dataset, producing a number of subbands. The decomposition procedure can be repeated recursively on one or more of the subbands to yield multiple levels of decomposition of lower and lower resolution.

The most commonly used multidimensional DWT structure consists of a recursive decomposition of the lowest-resolution subband. This *dyadic* decomposition structure is illustrated for a 2D image in Figure 1(a). In a 2D dyadic DWT, the original image is decomposed into four subbands each being one fourth the size of the original image, and the lowest-resolution subband (the *baseband*) is recursively decomposed. The dyadic transform structure is trivially extended to 3D imagery as illustrated in Figure 1(b)—a single stage of 3D decomposition yields 8 subbands with the baseband recursively decomposed for a 3D dyadic transform.

Alternative transform structures arise when subbands other than, or in addition to, the baseband are subjected to further decomposition. Generally referred to as *wavelet-packet* transforms, these decomposition structures can be fixed (like the dyadic structure), or be optimally adapted for each image coded (i.e., a so-called *best-basis* transform structure [4]). Packet transforms offer the potential to better match the spatial or spatiotemporal characteristics of certain imagery and can thereby at times yield greater coding efficiency. Although not widely used for 2D image coding,[1] fixed packet transforms, such as those illustrated in Figure 2, have been extensively deployed in 3D image coders and often yield coding efficiency substantially superior to that of the dyadic transform of Figure 1(b). In particular, the packet structure of Figure 2(a) has been shown to be near optimal in certain applications, producing coding performance nearly identical to the optimal packet decomposition structure chosen in a rate-distortion best-basis sense [6, 7].

Although there are many possible wavelet-transform filters, image-coding applications almost exclusively rely on the ubiquitous biorthogonal 9/7 transform of [14] or the simpler biorthogonal 5/3 transform of [15]. Biorthogonality facilitates symmetric extension at image boundaries and permits linear-phase FIR filters. Furthermore, experience has shown that the biorthogonal 9/7 offers generally good coding performance [16], while the biorthogonal 5/3 is attractive for reducing computational complexity or for implementation of reversible, integer-to-integer transformation [17, 18]. In fact, the biorthogonal 9/7 and an integer-valued biorthogonal 5/3 are the only transforms permitted by Part 1 of the JPEG2000 standard [13], although coding extensions of Part 2 [19] of the standard permit a greater variety of transforms.

2.1.2. Coding procedures

Many wavelet-based coders for 2D and 3D images are based on the following observations which tend to hold true for dyadic decompositions of many classes of imagery: (1) since most images are lowpass in nature, most signal energy is compacted into the lower-resolution subbands; (2) most coefficients are zero for high-resolution subbands; (3) small- or zero-valued coefficients (i.e., *insignificant coefficients*) tend to be clustered together within a given subband; and (4) clusters of insignificant coefficients in a subband tend to be located in the same relative position as similar clusters in the subband of the same orientation at the next higher-resolution level.

Wavelet-based image coders typically implement the following coding procedure. DWT coefficients are represented in sign-magnitude form with the signs and magnitudes coded separately. Coefficient magnitudes are successively approximated via *bitplane coding* wherein the most significant bit of all coefficient magnitudes is coded, followed by the next-most significant bit, and so forth. In practice,

[1] The WSQ fingerprint coding standard [5] is one example of a fixed packet transform in 2D.

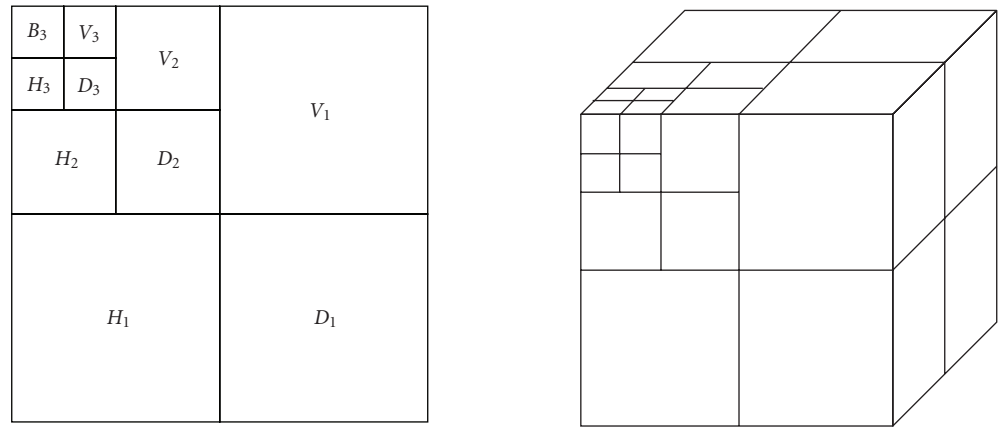

Figure 1: Dyadic DWT with three levels of decomposition. (a) 2D; (b) 3D.

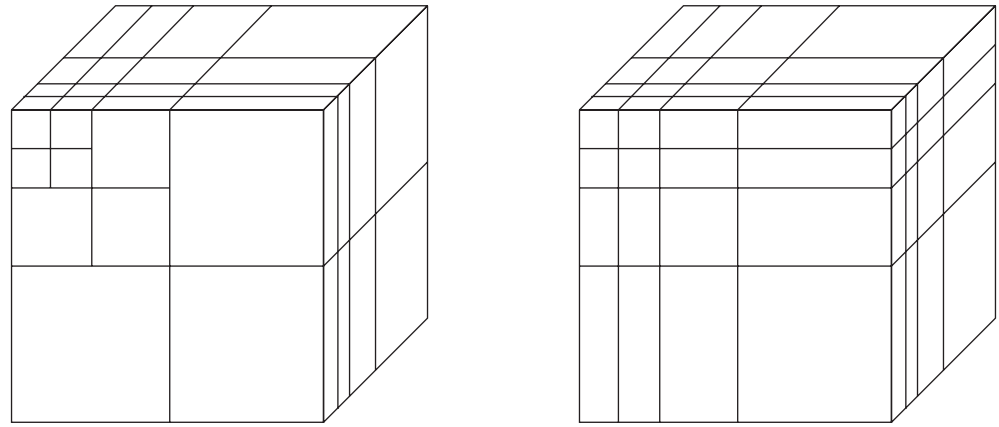

Figure 2: Examples of 3D wavelet-packet DWTs with three levels of decomposition. (a) 2D dyadic plus independent 1D dyadic; (b) three independent 1D dyadic transforms.

such bitplane coding is usually implemented by performing two coding passes through the set of coefficients for each bitplane—a *significance pass* and a *refinement pass*. In essence, the significance pass describes the first bitplane holding a nonzero bit for all the coefficients in the DWT while the refinement pass produces a successive approximation of each coefficient after its most significant nonzero bit is coded. The significance pass works by successively coding a map—the *significance map*—of coefficients which are insignificant relative to a threshold; the primary difference between wavelet-based coders lies in how this significance-map coding is performed. Table 1 presents an overview of prominent significance-map coding strategies which we discuss in detail below.

Zerotrees are one of the most widely used techniques for coding significance maps in wavelet-based coders. Zerotrees capitalize on the fact that, in dyadic transforms, insignificant coefficients tend to cluster together within a subband, and clusters of insignificant coefficients tend to be located in the same location within subbands of different resolutions. As illustrated in Figure 3(a), "parent" coefficients in a subband can be related to "children" coefficients in the same relative location in a subband at the next higher resolution. A *zerotree* is formed when a coefficient and all of its descendants are insignificant with respect to the current threshold. The embedded zerotree wavelet (EZW) algorithm [8] was the first image coder to make use of zerotrees. Later, the set partitioning in hierarchical trees (SPIHT) algorithm [9] improved upon the zerotree concept by adding a number of sorted lists that contain sets of coefficients (i.e., zerotrees) and individual coefficients. Both EZW and SPIHT were originally developed for 2D images. EZW has been extended to 3D in [20, 21]; SPIHT has been extended to 3D in [22–27]. Whereas extending the 2D zerotree structure to a 3D dyadic transform is simple, fitting zerotrees to the 3D packet transforms of Figure 2 is less straightforward. The

Table 1: Strategies for significance-map coding in wavelet-based still image coders.

Strategy	Prominent examples	Methodology	Notes
Zerotrees	EZW [8], SPIHT [9]	Cross-scale trees of coefficients plus arithmetic coding	Widely used
Set partitioning	SPECK [10, 11], BISK [12]	Set splitting into subsets plus arithmetic coding	No cross-subband processing
Conditional coding	JPEG2000 [13]	Multicontext arithmetic coding of small blocks; arithmetic coding; optimal block truncation	Superior rate-distortion performance; cross-subband processing confined to block-truncation process

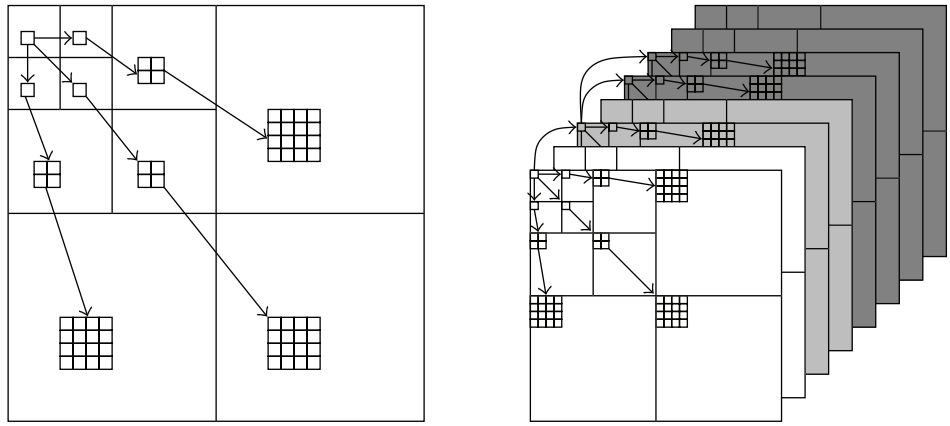

(a) (b)

Figure 3: Zerotrees in (a) the 2D dyadic transform of Figure 1(a), (b) the 3D packet transform of Figure 2(a).

asymmetric zerotree structure originating in [25] and illustrated in Figure 3(b) typically provides the best performance for the packet transform of Figure 2(a).

Despite the prominence of zerotree-based algorithms, recent work [28] has indicated that, typically, the ability to predict the insignificance of a coefficient through cross-scale parent-child relationships is somewhat limited compared to the predictive ability of neighboring coefficients within the same subband. Consequently, recent algorithms have focused on coding significance-map information using only within-subband information. An alternative to zerotrees for significance-map coding is within-band *set partitioning*. The set-partitioning embedded block coder (SPECK) [10, 11], originally developed as a 2D image coder, employs quadtree partitioning (see Figure 4(a)) to locate significant coefficients within a subband; a 3D extension (3D-SPECK [29, 30]) replaces quadtrees with octrees as illustrated in Figure 4(b). A similar approach is embodied by the binary set splitting with k-d trees (BISK) algorithm in both its 2D (2D-BISK [12]) and 3D (3D-BISK [3, 31]) variants wherein sets are always partitioned into two subsets. An advantage of these set-partitioning algorithms is that sets are confined to reside within a single subband at all times throughout the algorithm, whereas zerotrees span across multiple transform resolutions. Not only does this fact entail a simpler implementation, it is also beneficial from a computational standpoint as the coder must buffer only a single subband at a given time, leading to reduced dynamic memory needed [11]. Furthermore, the SPECK and BISK algorithms are easily applied to both the dyadic and packet transform structures of Figures 1(b), 2(a), and 2(b) with no algorithmic differences.

Another approach to within-subband coding is to employ extensively conditioned, multiple-context adaptive arithmetic coding. JPEG2000 [13, 19, 32–34], the most prominent *conditional-coding* technique, codes the significance map of an image using the known significance states of neighboring coefficients to provide the context for the coding of the significance state of the current coefficient. To code a 2D image, a JPEG2000 encoder first performs a 2D wavelet transform on the image and then partitions each transform subband into small, 2D rectangular blocks called codeblocks, which are typically of size 32×32 or 64×64 pixels. Subsequently, the JPEG2000 encoder independently generates an embedded bitstream for each codeblock. To assemble the individual codeblock bitstreams into a single, final bitstream, each codeblock bitstream is truncated in some fashion, and the truncated bitstreams are concatenated together to form the final bitstream.

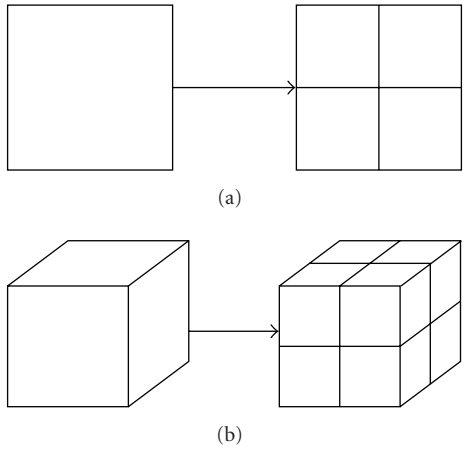

FIGURE 4: Set partitioning. (a) 2D quadtree partitioning. (b) 3D octree partitioning.

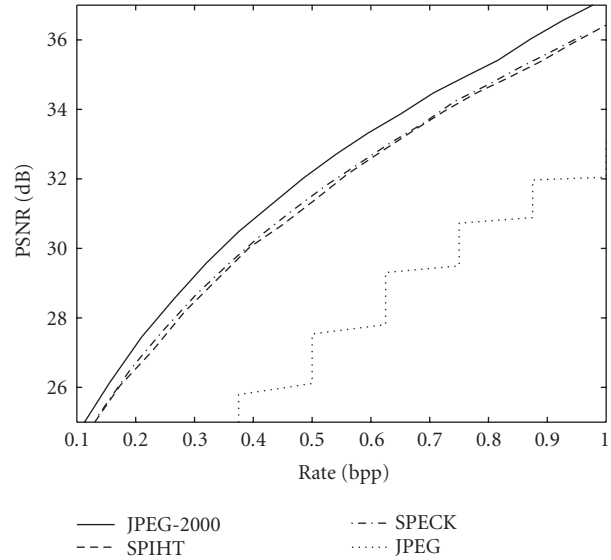

FIGURE 5: Rate-distortion performance for the 2D "barbara" image comparing the wavelet-based JPEG2000, SPIHT, and SPECK coders, as well as the original JPEG standard [38, 39]. The QccPack [40] (http://qccpack.sourceforge.net) implementations for SPIHT and SPECK are used, while JPEG-2000 is Kakadu Ver. 5.1 (http://www.kakadusoftware.com) and JPEG is the Independent JPEG Group implementation (http://www.ijg.org). The wavelet-based coders use a 5-stage wavelet decomposition with 9–7 wavelet filters.

In JPEG2000, the method for codeblock-bitstream truncation is typically a Lagrangian rate-distortion optimal technique, *post-compression rate-distortion (PCRD) optimization* [32, 35]. PCRD optimization is performed simultaneously across all of the codeblocks from the image, producing an optimal truncation point for each codeblock. The truncated codeblocks are then concatenated together to form a single bitstream. The PCRD optimization, in effect, distributes the total rate for the image spatially across the codeblocks in a rate-distortion-optimal fashion such that codeblocks with higher energy, which tend to more heavily influence the distortion measure, tend to receive greater rate. Additionally, the truncated codeblock bitstreams are interleaved in an optimal order such that the final bitstream is close to being rate-distortion optimal at many truncation points. As described in Part 1 of the standard, JPEG2000 is, in essence, a 2D image coder. However, for 3D imagery, the coding extensions available in Part 2 of the standard can effectuate the packet transform of Figure 2(a), and the PCRD optimization can be applied across all three dimensions; this strategy for 3D images has been called "JPEG2000 multicomponent" [36]. We note that JPEG2000 with truly 3D coding, consisting of arithmetic coding of 3D codeblocks as in [37], is under development as JPEG2000 Part 10 (JP3D), an extension to the core JPEG2000 standard; however, the use of JPEG2000 multicomponent currently remains widespread for 3D imagery. The reader is refered to [33, 34] for useful introductions to the JPEG2000 standard.

Figures 5 and 6 illustrate typical coding performance for some of the prominent 2D and 3D wavelet-based image coders discussed above. For 2D images, distortion is usually measured as a peak signal-to-noise ratio (PSNR), defined as

$$\mathrm{PSNR} = 10 \log_{10} \frac{255^2}{D}, \tag{1}$$

where D is the mean square error (MSE) between the original image and the reconstructed image; for 3D images, typically an SNR is used where 255^2 in (1) is replaced by the

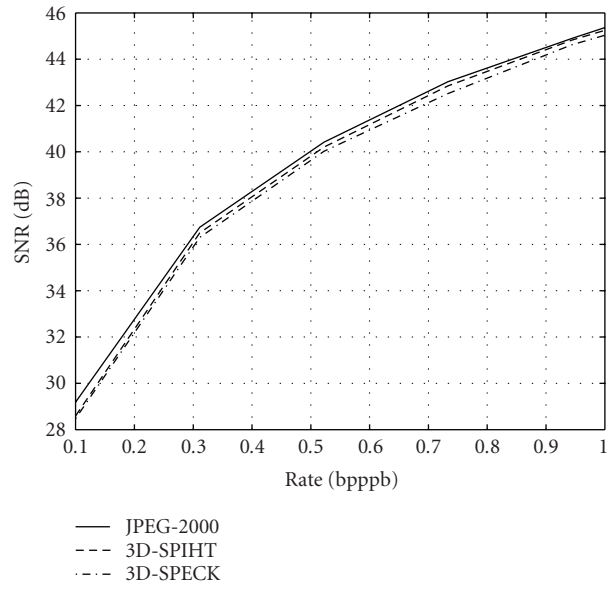

FIGURE 6: Rate-distortion performance for the 3D image "moffett," an AVIRIS hyperspectral image of spatial size 512×512 with 224 spectral bands. A wavelet-packet transform with 9–7 wavelet filters and 4 levels both spatially and spectrally is used. 3D-SPIHT uses asymmetric zerotrees, and JPEG2000-multicomponent cross-band rate allocation is used for JPEG2000.

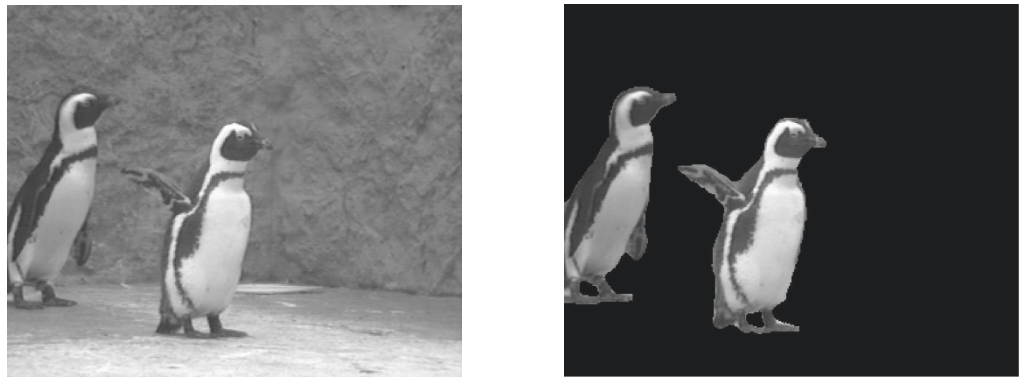

(a) (b)

Figure 7: (a) Original scene. (b) Arbitrarily shaped image objects to be coded with shape-adaptive coding.

dataset variance. Both the PSNR and SNR have units of decibels (dB). The bitrate is measured in terms of bits per pixel (bpp) for 2D images and typically bits per voxel (bpv) for 3D imagery (equivalently bits per pixel per band (bpppb) for hyperspectral imagery consisting of multiple spectral bands). We see in Figures 5 and 6 that JPEG2000 offers performance somewhat superior to that of the other techniques for both 2D and 3D coding.

In this special issue, the work "Adaptation of zerotrees using signed binary digit representations for 3D image coding" by E. Christophe et al. presents a 3D zerotree-based coder operating on hyperspectral imagery decomposed with the packet transform of Figure 2(a). The 3D-EZW algorithm is modified so as to eliminate the refinement pass (called the "subordinate" pass in the context of EZW [8]). Eliminating the subordinate pass, which typically entails a sorted list, simplifies the algorithm implementation but decreases coding efficiency. However, the use of a signed-binary-digit representation rather than the traditional sign-magnitude form for the wavelet coefficients increases the proportion of zero bits in the bitplanes, thereby increasing coding efficiency back to equal the original 3D-EZW implementation. Also **in this special issue**, "JPEG2000 compatible lossless coding of floating-point data" by B. E. Usevitch proposes extensions to the JPEG2000 standard to provide lossless coding of floating-point data such as that arising in many scientific applications. Several modifications to the JPEG2000 bitplane-coding procedure and context conditioning are made to accommodate extended-integer representation of floating-point numbers.

2.1.3. Coding of arbitrarily shaped imagery

In traditional image processing—as is the case in the preceding discussion—it is implicitly assumed that imagery has the shape of a rectangle (in 2D) or rectangular volume (in 3D). The majority of image-coding literature addresses the coding of only rectangularly shaped imagery. However, imagery with arbitrary, nonrectangular shape has become important in a number of areas, including multimedia communications (e.g., the arbitrarily shaped video objects as covered by the MPEG-4 video-coding standard [41] and other approaches [42–47]), geospatial imagery (e.g., oceanographic temperature datasets [3, 31, 48, 49], multispectral/hyperspectral imagery [50, 51]), and biomedical applications (e.g., mammography [52], DNA microarray imagery [53–55]). *Shape-adaptive image coding* for these applications is usually achieved by adapting existing image coders designed for rectangular imagery to the shape-adaptive coding problem.

In a general sense, shape-adaptive coding can be considered to be the problem of coding an arbitrarily shaped imagery "object" residing in a typically rectangularly shaped "scene" as illustrated in Figure 7. The goal is to code the image object without expending any bits towards the nonobject portions of the scene. Typically, an object "mask" will be required to be transmitted to the decoder separately in order to delineate the object from nonobject regions of the scene. Below we focus on object coding alone, assuming that any one of a number of lossless bilevel-image coding algorithms is used to provide an efficient representation of this binary object mask as side information to the central shape-adaptive image-coding task. Likewise, the segmentation of image objects from the nonobject background is considered an application-specific issue outside the scope of the shape-adaptive coding problem.

As discussed above, typical wavelet-based coders have a common design built upon three major components—a DWT, significance-map coding, and successive-approximation quantization in the form of bitplane coding. Each of these constituent processes is easily rendered shape adaptive for the coding of an image object with arbitrary shape. Typically, a *shape-adaptive DWT* (SA-DWT) [42] is employed such that only image pixels lying inside the object are transformed into wavelet coefficients. Once in the wavelet domain, all regions corresponding to nonobject areas in the original image are permanently considered "insignificant" and play the same role as true insignificant coefficients in significance-map coding. While most shape-adaptive coders are based on this general idea, a number of approaches employ various modifications to the significance-map encoding

(such as explicitly discarding sets consisting of only nonobject regions from further consideration [3, 12, 31, 43, 44]) to increase performance. See [3] for a comprehensive overview of wavelet-based shape-adaptive coders.

In this special issue, the work "Costs and advantages of object-based image coding with shape-adaptive wavelet transform" by M. Cagnazzo et al. examines sources of inefficiencies as well as sources of performance gains that result from the application of shape-adaptive coding. It is observed that inefficiencies arise from both the reduced energy-compaction capabilities of the SA-DWT (due to less data for the DWT to process) as well as an interaction of the significance-map coding with object boundaries (e.g., in shape-adaptive SPIHT [43], zerotrees which overlap the object/nonobject boundary). On the other hand, image objects tend to be more coherent and "smoother" than full-frame imagery since object/nonobject boundary edges are not present in the object, a characteristic that may lead to coding gains. Experimental results in "Costs and advantages of object-based image coding with shape-adaptive wavelet transform" by M. Cagnazzo et al. provide insight as to the relative magnitude of these losses and gains as can be expected in various operational conditions.

2.2. Video coding

The outstanding rate-distortion performance of the coders described above has led to wavelets dominating the field of still-image compression over the last decade. However, such is not the case for wavelets in video coding. On the contrary, the traditional architecture (illustrated in Figure 8) consisting of a feedback loop of block-based *motion estimation* (ME) and *motion compensation* (MC) followed by a *discrete cosine transform* (DCT) of the residual is still widely employed in modern video-compression systems and an integral part of standards such as MPEG-2 [59], MPEG-4 [41], and H.264/AVC [60]. However, there has naturally been great interest in carrying over the gains seen by wavelet-based still-image coders into the video realm, and several different approaches have been proposed. The first, and most straightforward, is essentially an adaptation of the traditional ME/MC feedback architecture to the use of a DWT, employing a redundant transform to provide the shift invariance necessary to the wavelet-domain ME/MC process. A second approach involves eliminating the feedback loop of the traditional architecture by applying ME/MC in an "open-loop" manner to drive a temporal wavelet filter. Finally, a recent strategy proposes eliminating explicit ME/MC altogether and instead relying on the greater directional sensitivities of a 3D complex wavelet transform to represent the motion of signal features. Table 2 overviews each of the these recent approaches to wavelet-based video coding, and we discuss each one in detail below.

2.2.1. Redundant transforms and video coding

Perhaps the most straightforward approach to wavelet-based video coding is to simply replace the DCT with a DWT in the traditional architecture of Figure 8, thereby performing ME/MC in the spatial domain and calculating a DWT on the resulting residual image (e.g., [61]). This simple approach suffers from blocking artifacts [62], which are exacerbated if the DWT is not block based but rather the usual whole-image transform. An alternative paradigm would be to have ME/MC take place in the wavelet domain (e.g., [63]). However, the fact that the critically sampled DWT used ubiquitously in image-compression efforts is shift variant has long hindered the ME/MC process in the wavelet domain [64, 65].

It was recognized in [56, 66, 67] that difficulties associated with the shift variance of traditional DWTs could be overcome by choosing instead to perform ME/MC in the domain of a redundant transform. In essence, the *redundant DWT* (RDWT)[2] [69–71] removes the downsampling operation from the traditional DWT to ensure shift invariance at the cost of a redundant, or overcomplete, representation.

There are several equivalent ways to implement the RDWT, and several ways to represent the resulting overcomplete set of coefficients. The most popular coefficient-representation scheme employed in RDWT-based video coders is that of a coefficient tree. This tree representation is created by employing filtering and downsampling as in the usual critically sampled DWT; however, all sets, or phases, of downsampled coefficients are retained and arranged in a tree-like fashion. The RDWT was originally formulated, however, as the *algorithme à trous* implementation [69, 70]. In this implementation, decimation following wavelet filtering is eliminated, and, for each successive scale of decomposition, the filter sequences themselves are upsampled, creating "holes" of zeros between nonzero filter taps. As a result, the size of each subband resulting from an RDWT decomposition is exactly the same as that of the input signal, as is illustrated for a 2D image in Figure 9. By appropriately subsampling each subband of an RDWT, one can produce exactly the same coefficients as does a critically sampled DWT applied to the same input signal.

The majority of a prior work concerning RDWT-based video coding originates in the work of Park and Kim [56], in which the system shown in Figure 10 was proposed. In essence, the system of Figure 10 works as follows. An input frame is decomposed with a critically sampled DWT and partitioned into cross-subband blocks, wherein each block is composed of the coefficients from each subband that correspond to the same spatial block in the original image. A full-search block-matching algorithm is used to compute motion vectors for each wavelet-domain block; the system uses as the reference for this search an RDWT decomposition of the previous reconstructed frame, thereby capitalizing on the shift invariance of the redundant transform. Any of the 2D image coders described above in Section 2.1.2 is then used to code the MC residual. Subsequent work has offered refinements to the system depicted in Figure 10, such as the deriving of motion vectors for each subband [72, 73], or resolution

[2] There are several names that have been given to this transform, including the overcomplete DWT (ODWT) and the undecimated DWT (UDWT)—our use of the RDWT moniker is from [68].

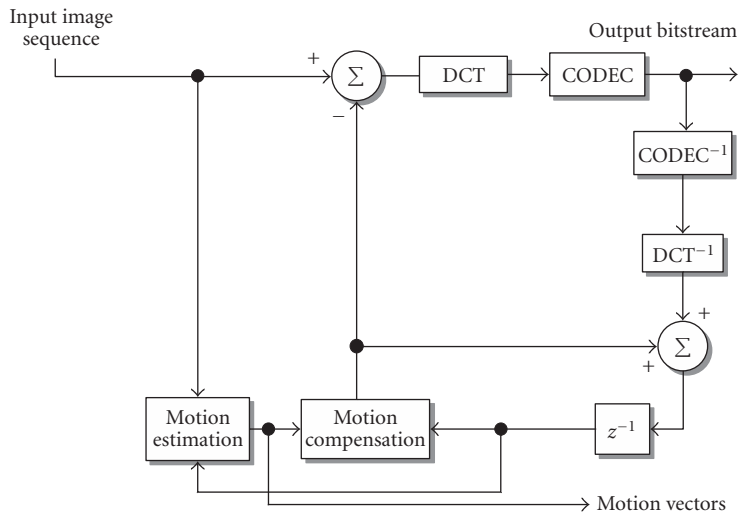

Figure 8: The traditional video-coding system consisting of ME/MC followed by DCT. z^{-1} = frame delay, *CODEC* is any 2D still-image coder.

Table 2: Strategies for wavelet-based video coding.

Strategy	Prominent examples	Methodology	Notes
Wavelet-based hybrid coding	Park and Kim [56]	ME/MC in wavelet domain via shift-invariant RDWT	
MCTF	MC-EZBC [57]	Temporal transform eliminates ME/MC feedback loop	Performance competitive with traditional coders (H.264); full scalability
Complex wavelet transforms	[58]	Directionality of transform eliminates ME/MC	Performance between that of 3D still-image coding and traditional hybrid coding; no ME/MC

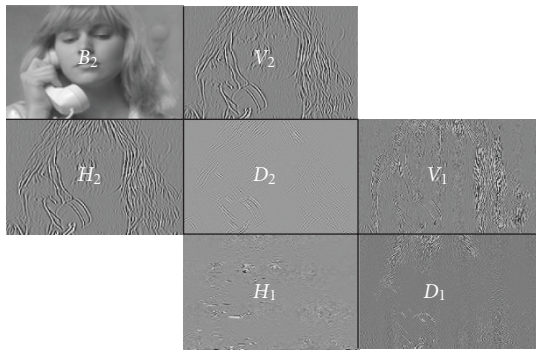

Figure 9: Spatially coherent representation of a two-scale RDWT of a 2D image. Coefficients retain their correct spatial location within each subband, and each subband is the same size as the original image. B_j, H_j, V_j, and D_j denote the baseband, horizontal, vertical, and diagonal subbands, respectively, at scale j.

[74], independently; subpixel accuracy ME [75, 76]; and resolution-scalable coding [73, 74, 77].

In most of the RDWT-based video-coding systems described above, the redundancy inherent in the RDWT is used exclusively to permit ME/MC in the wavelet domain by overcoming the well-known shift variance of the critically sampled DWT. However, the RDWT redundancy can be put to greater use, as was demonstrated in [81, 82], wherein the redundancy of the RDWT is used to guide mesh-based ME/MC via a cross-subband correlation operator, and in [83, 84], wherein the transform redundancy is employed to yield multiple predictions diverse in transform phase that are combined into a single multihypothesis prediction.

2.2.2. Motion-compensated temporal filtering (MCTF)

Given the fact that wavelets are inherently suited to scalable coding, it is perhaps natural that the most widespread use of wavelets in video has occurred in conjunction with efforts to produce coders with a high degree of spatial, temporal, and fidelity scalability. It is thought that such scalability will be useful in numerous video-based communication applications, allowing a heterogeneous mix of receivers with varying capabilities to receive a single video signal, decoding at the spatial resolution, frame rate, and quality appropriate to the receiving device at hand. However, it has been generally recognized that the goal of highly scalable video representation

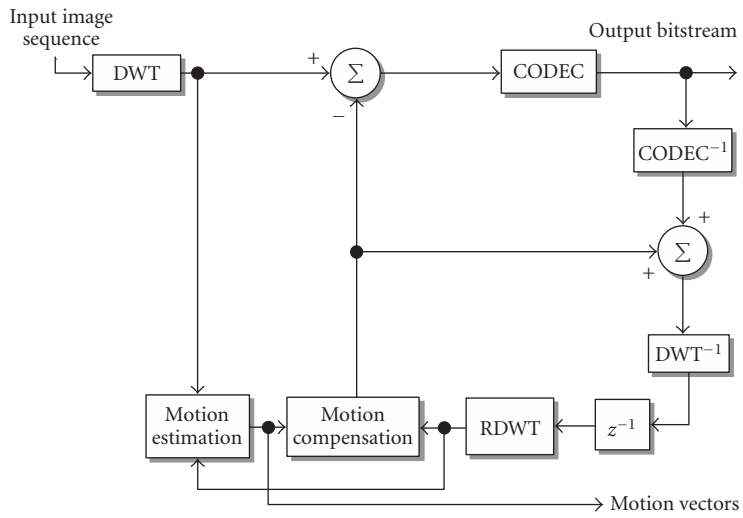

Figure 10: The RDWT-based video coder of [56]. z^{-1} = frame delay, *CODEC* is any still-image coder operating in the critically sampled-DWT domain as described in Section 2.1.2. The cascade of the inverse DWT and forward RDWT in the feedback loop can be computationally simplified by using a complete-to-overcomplete transform [78–80].

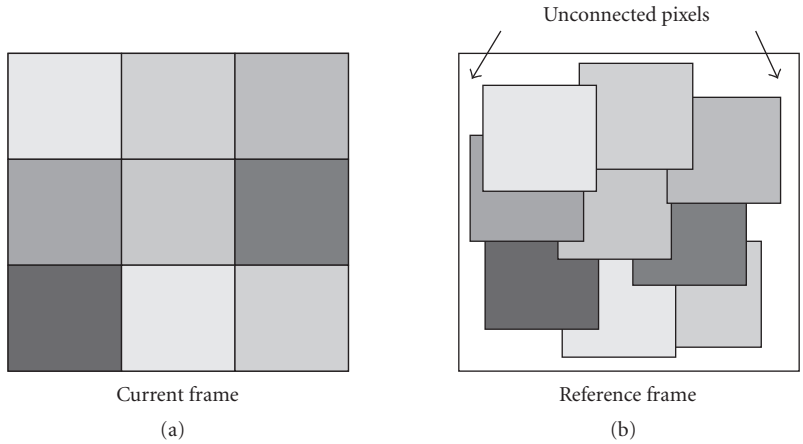

Figure 11: In MCTF using block matching, blocks in the reference frame corresponding to those in the current frame typically overlap. Thus, some pixels in the reference frame are mapped several times into the current frame while other pixels have no mapping. These latter pixels are "unconnected."

is fundamentally at odds with the traditional ME/MC feedback loop (such as in Figures 8 and 10) which hinders the achieving of a high degree of scalability. Consequently, 3D transforms, which break the ME/MC feedback loop, are a primary focus in efforts to provide full scalability. However, the deploying of a transform in the temporal direction without MC typically produces low-quality temporal subbands with significant "ghosting" artifacts [85] and decreased coding efficiency. Consequently, there has been significant interest in *motion-compensated temporal filtering* (MCTF) in which it is attempted to have the temporal transform follow motion trajectories. Below, we briefly overview MCTF and its recent use in wavelet-based video coding; for a more thorough introduction, see [86, 87].

Many approaches to MCTF follow earlier works [88, 89] which adapted block-based ME/MC to the temporal-transform setting, that is, video frames are divided into blocks, and motion vectors of the blocks in the current frame point to the closest matching blocks in the preceding reference frame. If there is no motion, or there is only pure translational motion, the motion vectors provide a one-to-one mapping between pixels in the reference frame and pixels in the current frame. This one-to-one mapping between frames then provides the trajectory for filtering in the temporal direction for MCTF. However, in more realistic video sequences, motion is usually much more complex, yielding one-to-many mappings for some pixels in the reference frame and no mapping for others, such as illustrated in

Figure 11. These latter pixels are thus "unconnected" and are handled in a typically *ad hoc* manner outside of the temporal-filtering process, while a single temporal path is chosen for multiconnected pixels typically based on raster-scan order.

It has been recognized that a *lifting*[3] implementation [90, 91] permits the MC process in the temporal filtering to be quite general and complex while remaining easily inverted. For example, let $x_1(m,n)$ and $x_2(m,n)$ be two consecutive frames of a video sequence, and let $W_{i,j}$ denote the operator that maps frame i onto the coordinate system of frame j through the particular MC scheme of choice. Ideally, we would want $W_{1,2}[x_1](m,n) \approx x_2(m,n)$. Haar-based MCTF would then be implemented via lifting as

$$\begin{aligned} h(m,n) &= \frac{1}{2}\left(x_2(m,n) - W_{1,2}[x_1](m,n)\right), \\ l(m,n) &= x_1(m,n) + W_{2,1}[h](m,n), \end{aligned} \tag{2}$$

where $l(m,n)$ and $h(m,n)$ are the lowpass and highpass frames, respectively, of the temporal transform [91]. This formulation, illustrated in Figure 12, permits any MC to be used since the lifting decomposition is trivially inverted as

$$\begin{aligned} x_1(m,n) &= l(m,n) - W_{2,1}[h](m,n), \\ x_2(m,n) &= 2h(m,n) + W_{1,2}[x_1](m,n). \end{aligned} \tag{3}$$

The lifting implementation of the temporal filtering facilitates temporal filters longer than the Haar [91–93], subpixel accuracy for ME [57, 90, 91, 94–96], bidirectional MC and multiple reference frames [57, 96, 97], multihypothesis MC [98–101], ME/MC using meshes rather than blocks [85, 95, 100, 101], and multiple-band schemes that increase temporal scalability [102–104].

For coding, MCTF is combined with a 2D spatial DWT, and typically one of the 3D coders described in Section 2.1.2, such as 3D-SPIHT or JPEG2000 multicomponent, is applied to render the final bitstream. In the absence of MC, the temporal transform would be applied separately from the spatial transform, resulting in the packet decomposition of Figure 2(a). In such a case, the order in which the temporal and spatial transforms were performed would not matter. However, due to the shift invariance of the spatial DWT in the presence of MC, the temporal and spatial transforms do not commute, giving rise to two broad families of MCTF architectures.

Most MCTF-based coders apply MCTF first on spatial-domain frames, following with a spatial 2D dyadic DWT. Such "$t + 2D$" coders have the architecture illustrated in Figure 13(a). A number of prominent MCTF-based coders (e.g., [57, 88–98, 105]) employ the t+2D architecture, including the prominent MC-EZBC coder [57]—currently largely considered to be the state-of-the-art in wavelet-based MCTF scalable coding—and its refinements [105–107]. Alternatively, one can reverse the transform order, applying the spatial transform first, and then conducting temporal filtering among wavelet-domain frames. Such "2D+t" coders [76, 99–101, 108–111] typically apply MCTF within each subband (or resolution) independently as illustrated in Figure 13(b); a spatial RDWT such as described in Section 2.2.1 is often used to provide shift invariance for the wavelet-domain MCTF. Finally, a hybrid "$2D + t + 2D$" architecture was proposed in [86, 112, 113] to continuously adapt between the $t + 2D$ and $2D + t$ structures to reduce motion artifacts under both temporal and spatial scaling.

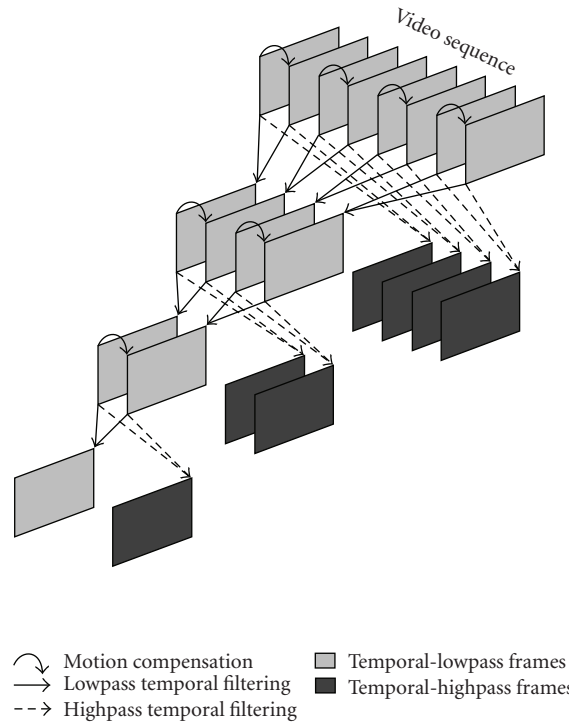

Figure 12: Haar-based MCTF, depicting three levels of temporal decomposition.

We note that the forthcoming extension to H.264/AVC for scalable video coding [114, 115] uses open-loop ME/MC for temporal scalability and is closely related in this sense to MCTF. However, the remainder of the coder follows a more traditional layered approach to scalability with an H.264/AVC-compatible base layer. An oversampled pyramid, rather than a spatial DWT, is used for spatial scalability.

In this special issue, it is recognized in "Quality variation control for three-dimensional wavelet-based video coders" by V. Seran and L. P. Kondi that different temporal-filter synthesis gains between even and odd frames lead to fluctuations in quality from frame to frame in the reconstructed video sequence for both the $t + 2D$ and $2D + t$ MCTF architectures. Two approaches are proposed in the same paper for dealing with the temporal quality variation: a rate-control algorithm that sets appropriate priorities for the temporal subbands as well as an approach to modify the filter coefficients directly to compensate for the fluctuation. Also in this issue, a t+2D coder that produces a JPEG2000 bitstream (using the Part 3 [116], "motion JPEG2000," component of the

[3] See Section 2.3 for more on lifting in general.

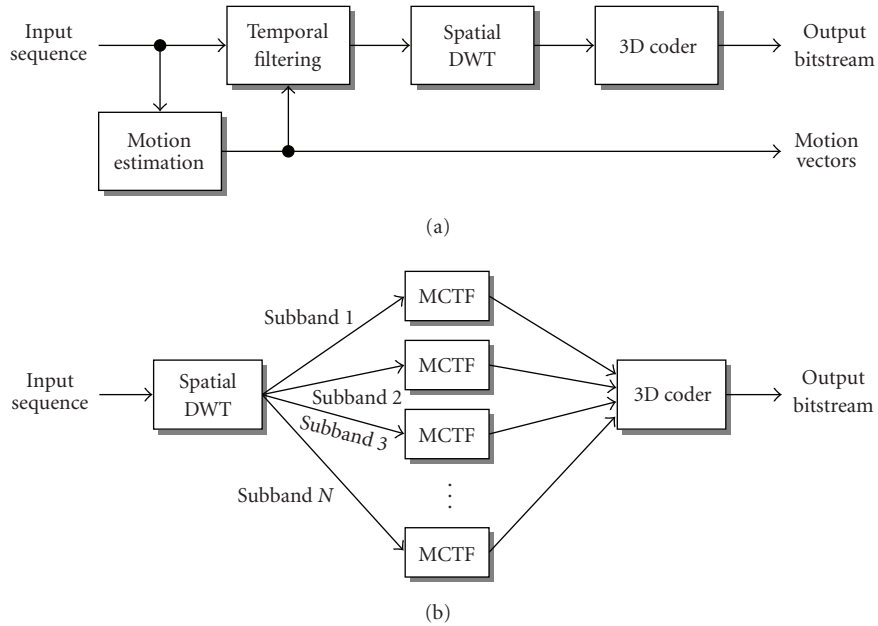

FIGURE 13: (a) The $t+2D$ MCTF architecture. (b) The $2D+t$ MCTF architecture, with "in band" MCTF applied individually on each spatial subband. "3D coder" indicates any of the 3D wavelet-based coders from Section 2.1.2.

standard) is proposed in [117]. In this coder, a model-based bit-allocation procedure is designed to yield a high degree of scalability.

2.2.3. Complex wavelet transforms

Although MCTF as discussed above is a relatively recent innovation, the concept of coding video by grouping several frames together into a 3D volume and employing transforms in the spatial and temporal directions has been explored on and off in the literature for the past several decades—an early wavelet-based example is [118]. However, temporal transforms for video pose a unique problem that causes 3D video coding to be different from the coding of other 3D data types; MCTF is just one approach to temporally decorrelating object pixels regardless of the frame-to-frame motion they undergo. An alternative to MCTF has arisen recently in the form of the complex *dual-tree discrete wavelet transform* (DDWT) [119–121]. The DDWT is a redundant transform that, in the 3D case [121], produces four times as many subbands as the DWT, with each subband oriented in a different spatiotemporal direction. When applied to a video signal, these orientations help isolate image features moving in different directions, providing inherent motion selectivity. The ability of the transform to describe motion without explicit ME/MC has motivated the use of the DDWT in video-coding systems [58, 122] looking to avoid the computational complexity associated with ME. However, since the 3D DDWT is four times redundant, efficient coding of the transform coefficients is a challenging task.

In this special issue, "Video coding using 3D dual-tree wavelet transform" by B. Wang et al. as well as in preceding work [58], a DDWT-based video coder is proposed to exploit the fact that a significant degree of correlation exists between DDWT coefficients residing at the same spatiotemporal locations in different subbands. Twenty-eight-dimensional cross-subband vectors of DDWT coefficients assembled from the 28 highpass DDWT subbands are assembled and coded with arithmetic coding resulting in rate-distortion performance superior to that of 3D-SPIHT [22, 23] applied directly to a 3D DWT of the video sequence with no ME or MC. In [124], it is further recognized that large-magnitude DDWT coefficients occur rather sparsely such that small or zero coefficients tend to form spatiotemporally coherent regions within each subband. A coder is then proposed which combines the BISK algorithm [3, 12, 31], the packet transform of Figure 2(b), and 4-dimensional cross-subband vectors of DDWT coefficients.

2.3. Image-adaptive lifting transforms

The 2D and 3D image coders discussed above rely on the DWT applied to the image data to result in coefficients having, more or less, the properties outlined at the start of Section 2.1.2. Although traditional DWTs do a reasonably good job at this task, there have been a number of efforts to improve wavelet decompositions by abandoning their fixed structure in favor of transforms that adapt to local signal characteristics. For this, an alternative transform implementation is essential.

DWTs have long been understood, and implemented, in terms of filter banks, and several early approaches at signal-adaptive transforms proposed nonstationary filter-based decompositions (e.g., [125, 126]). However, recent use has favored implementations based on *lifting* [123, 127]. It is well known that any biorthogonal DWT can be factored

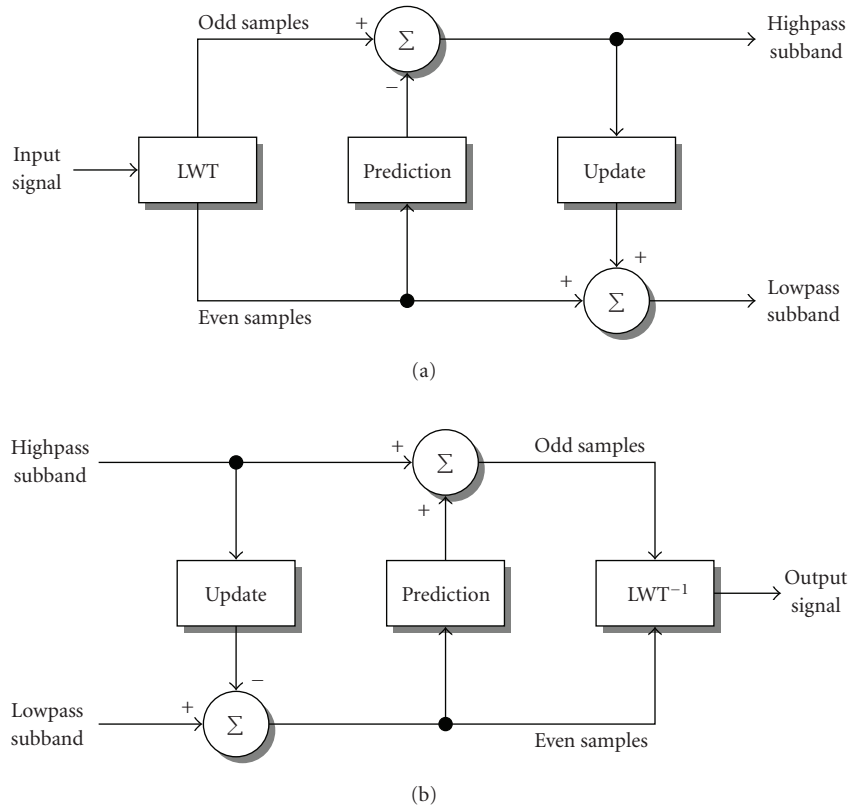

Figure 14: A 1D DWT implemented via lifting. (a) The forward transform (analysis). (b) The inverse transform (synthesis). LWT is a polyphase decomposition of the input signal into even-indexed and odd-indexed samples (the "lazy wavelet transform" [123]).

into a sequence of lifting steps, typically resulting in an implementation with computational complexity significantly reduced as compared to the traditional convolution-based filter-bank implementation [128]. This fact alone would account for widespread use in practical DWT implementations; however, the lifting structure, depicted in Figure 14, permits a number of interesting generalizations to the DWT via suitably modifying the prediction or update operators. Such "second-generation" wavelet constructs include boundary wavelets, wavelets on irregular sampling, and wavelets that map integers to integers [17, 18]; see [129] for an extensive overview of both first- and second-generation wavelets based on lifting.

The key to second-generation lifting formulations is that the inverse transform is trivially effectuated by simply reversing the operations of the forward transform, as illustrated in Figure 14(b). This fact has been exploited recently in order to devise transforms that *adapt* to local signal features by modifying the prediction or update operations in response to local signal characteristics [130–146]. In these schemes, as long as the inverse transform can track the prediction/update variations made by the forward transform, perfect reconstruction is assured. Such *signal-adaptive* transforms clearly lack shift invariance and are typically nonlinear, but often produce subband signals that can be better exploited in applications. Of primary interest are schemes that permit adaption to take place without the need for "side information" between the forward and inverse transforms. Although explicitly describing the adaption decisions made at the forward transform permits easy implementation of the inverse transform, the side information results in a transform that is, in essence, no longer critically sampled but, rather, overcomplete.

The most common approach to adaptive lifting is based on the idea that highpass DWT subbands should be relatively sparse to be beneficial in most applications. As a consequence, the usual strategy is to design the prediction operator to adapt to the signal locally so as to minimize the energy in the resulting highpass subband. The update step, on the other hand, usually remains fixed, typically set to the update operator for some first-generation biorthogonal transform, such as that of the 5/3 DWT. This *adaptive-prediction* lifting strategy, employed in [130–136, 146], is illustrated in Figure 15. Alternatively, in [137–145], the opposite approach of an adaptive update operator plus fixed prediction is pursued; in this *adaptive-update* case, a large signal gradient produces a "weak" update step such that edges and other sharp signal features are not smoothed but retain their sharpness.

In order to permit trivial transform inversion of an adaptive-lifting scheme, the adaptive operator must operate on the same polyphase signal component as is used to drive the adaption of the operator itself. For example, as shown in

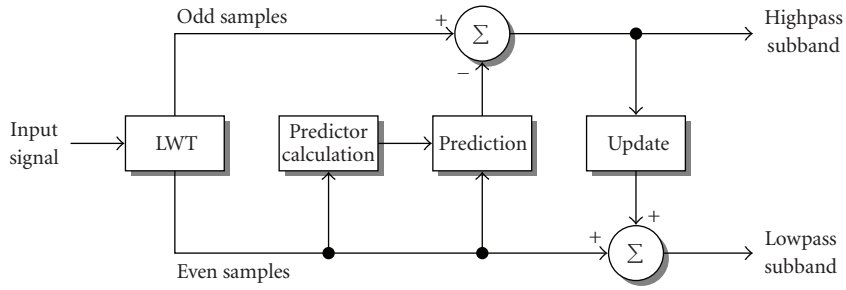

FIGURE 15: Adaptive-prediction lifting. Predictor is adapted to local signal features, usually in an effort to minimize energy in the highpass subband.

Figure 15, the adaption of the predictor operator is driven by the even polyphase component, and the predictor produces its prediction from the same even samples. In this manner, the predicted values, as well as the predictor itself, can be determined within the inverse transform. Most adaptive-lifting schemes follow this polyphase-based approach. However, the adaption of the predictor in [135, 136] is driven from the highpass subband (the opposite polyphase component); this adaption is based causally on already processed highpass coefficients such that the inverse transform can produce the same adaption. Additionally, the adaption of the update operator in [137–145] is driven from both polyphase components; in this case, the adaption is carefully designed mathematically to ensure perfect reconstruction.

In any case, the key to inversion of an adaptive lifting transform is having the inverse produce the same adaptive operator as did the forward transform. Clearly, any signal-processing operations—in particular, quantization—that lie between the forward transform and its inverse can jeopardize the ability to track the adaption of the operator in question. As a consequence, much of the prior literature considers only the application of lossless compression in conjunction with adaptive lifting (e.g., [132, 133, 144, 146]). On the other hand, lossy compression can be considered if one is mindful of the consequences that quantization can entail within the adaption process of the inverse transform. For example, in [130, 131], the adaptive-prediction step follows the fixed update step (contrary to the architecture of Figure 15), and the adaption of the predictor is driven by *quantized* signal values; in [135], quantization is applied within the feedback loop of the causal highpass prediction update; and, in [142, 143, 145] conditions are determined for recovering the original adaption decisions at the inverse transform, and a relation between the reconstruction error and the quantization error is derived.

To this point, we have considered issues surrounding adaptive lifting of 1D signals. For 2D imagery, the typical approach is to apply a 1D adaptive-lifting scheme such as depicted in Figure 15 separably to the rows and columns of the image. The 1D-based strategy can be further refined for 2D coding by enlarging the prediction (or update) context to include samples for rows/columns other than the current one [130, 131, 135, 136]. Alternatively, a quincunx subsampling scheme (see Figure 16) permits lifting to be applied in a nonseparable fashion directly in 2D [133, 146–149]; in this case, each lifting stage produces a single lowpass and a single highpass subband rather than the four directional subbands that arise in a separable DWT. Finally, the four directional subbands of the separable decomposition can be produced simultaneously via a single update operator combined with three prediction operators [138].

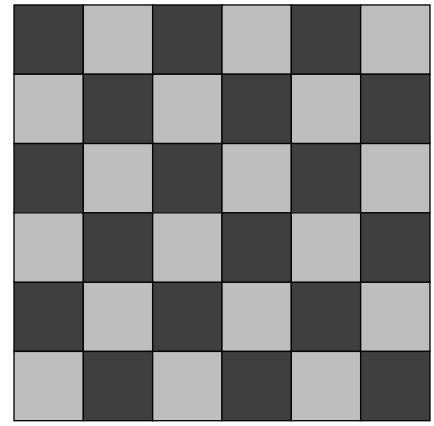

FIGURE 16: Quincunx subsampling. The two shades of gray indicate the two polyphase components.

In this special issue, the work "Block-based adaptive vector lifting schemes for multichannel image coding" by A. Benazza-Benyahia et al. proposes a vector-valued adaptive-lifting scheme in which a predictor is adapted on a block-by-block basis to the signal within quincunx-based lifting. Although the transform is overcomplete in that prediction-adaption decisions are explicitly transmitted to the inverse transform, the adaption decisions are conveyed simultaneously with the quadtree-based coding of the transform coefficients. In "An edge-sensing predictor in wavelet lifting structures for lossless image coding" by Ö. N. Gerek and A. E. Çetin, an adaptive prediction is designed in order to detect edge orientation and to form predictions accordingly; a 2D window is employed to determine edge orientation. Finally, in [150], the adaptive image-interpolation scheme of [151] is used as the basis of adaptive predictors and updates for

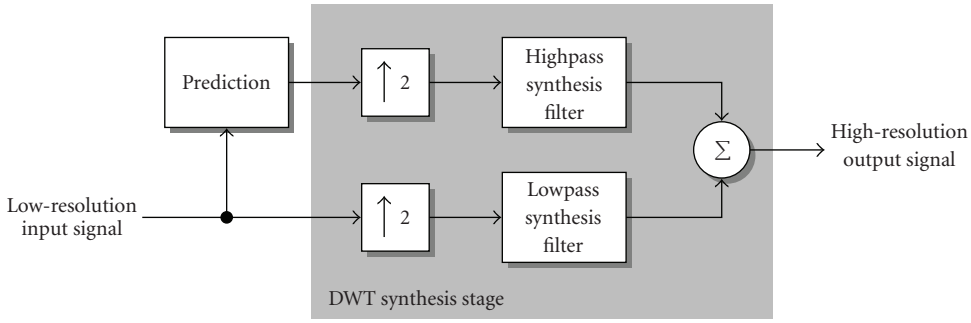

Figure 17: Wavelet-based interpolation of a 1D signal. 2D image interpolation may be accomplished by a similar system applied to the subbands of a 2D DWT synthesis stage, or by applying this 1D system in a separable fashion to image rows and columns independently.

lifting, and an application to lossless image compression is considered.

2.4. Image interpolation

Although wavelets have perhaps played their most prominent role in source-coding applications such as the image and video coders described above, wavelet-based signal representations are widely used in other applications, such as signal filtering, denoising, feature detection, and signal enhancement. In particular, the multiresolution characteristic inherent to wavelet transforms makes them a natural choice for the task of image interpolation—the magnification or resolution enhancement of an image with the goal of no loss to the sharpness of the image. The philosophy fundamental to wavelet-based image interpolation is illustrated in 1D in Figure 17. Essentially, a highpass subband is synthesized by a prediction process from the given low-resolution signal which is, itself, treated as a lowpass subband. Both subbands then undergo a single stage of DWT synthesis, resulting in a high-resolution signal magnified by a factor of 2 as compared to the original input signal.

Although image interpolation is a classic problem in the field of image processing, traditional solutions such as bilinear or bicubic interpolation impose a constraint on continuity in the image, resulting in a tendency to produce oversmoothed edges [152]. Additionally, these traditional interpolators include the original image pixels in the interpolated output image, essentially making an inherent assumption that the original low-resolution input image was produced by direct downsampling of some higher-resolution image. Yet, antialiasing filters are often used in practice in image acquisition or resolution reduction [152]. On the other hand, the inclusion of the lowpass synthesis filter in Figure 17 can be seen as compensating for the antialiasing filter (which would be the lowpass analysis filter in a nonexistent DWT analysis stage), while the predictor in Figure 17 explicitly adds high-frequency information to retain sharp edge and texture details.

Many wavelet-based interpolation schemes are based on the techniques originating in [153–155]. In these algorithms, a 1D RDWT (see Section 2.2.1) is used to determine edge locations in an image row or column by identifying signal features that persist across wavelet scales in accordance with the theory of [156]. The highpass band is then synthesized by "copying" signal features from a lower-resolution subband into the new highpass band at the locations of the identified edges. The regularity of the edges is preserved by measuring the decay in regularity across scales at the edge locations and extrapolating into the newly created highpass subband. This basic strategy has been enhanced by projection onto convex sets (POCS, e.g., [157]) to iteratively refine the initial extrapolated highpass band [153, 154]. Additionally, alternative strategies for producing the highpass prediction were proposed in the form of linear minimum mean square estimation [152], hidden Markov models [158], hidden Markov trees [159], and Gaussian mixture models [160].

In this special issue, the work "Image resolution enhancement via data-driven parametric models in the wavelet space" by X. Li adopts a POCS strategy consisting of an observational constraint (DWT analysis applied to the high-resolution interpolator output must match the original low-resolution input) as well as several additional constraints on sharp highpass signal features. Specifically, separate constraints are formulated for edges, contours, and texture features.

3. WAVELETS IN COMMUNICATIONS AND NETWORKING

In a typical communication scheme, the output of a source coder must be protected against errors caused by channel noise. Traditionally, this protection is accomplished by adding redundancy to the output of the source coder through channel coding, that is, via some form of error-correcting code. The traditional paradigm is to conduct the design of the source and channel coders separately from each other, concatenating the two once they have been independently optimized. However, it turns out that the overall concatenated system is typically optimal only under idealized conditions. As a consequence, several alternative strategies have arisen for producing the added redundancy necessary for

error-resilient communication, and wavelets have played a role in a number of them. Below, we survey the use of wavelets in the communication and networked transmission of images and video. First, in Section 3.1, we overview procedures that produce redundancy by creating multiple correlated codings, or descriptions, of the imagery for transmission across separate network paths. Then, in Section 3.2, we overview techniques that dispense with the assumption of the separability of the source and channel design problems to develop systems in which the source and channel coders are jointly designed.

3.1. Multiple-description coding

With increasing use of the Internet and other best-effort networks for multimedia communication, there is a growing need for reliable transmission. Traditional research efforts have concentrated on enhancing existing error-correction techniques; however, recent years have seen an alternative solution emerge and garner increasing attention. This latter solution focuses mainly on the situation in which immediate data retransmission is either impossible (e.g., network congestion or broadcast applications) or undesirable (e.g., conversational applications with very low delay requirements). We are referring to a specific technique known as *multiple-description coding* (MDC). In this section, we overview the use of wavelets in MDC; the reader is referred to [161] for a comprehensive general review of MDC.

In essence, the MDC technique operates as illustrated in Figure 18. The MDC encoder produces several correlated—but independently decodable—bitstreams called *descriptions*. The multiple descriptions, each of which preferably has equivalent quality, are sent over as many independent channels to an MDC decoder consisting of a *central decoder* as well as multiple *side decoders*. Each of the side decoders is capable of decoding its corresponding description independently of the other descriptions, producing a representation of the source with some level of minimally acceptable quality. On the other hand, the central decoder can jointly decode multiple descriptions to produce the best-quality reconstruction of the source. In the simplest scenario, the transmission channels are assumed to operate in a binary fashion; that is, if an error occurs in a given channel, that channel is considered damaged, and the entirety of the corresponding bitstream is considered unusable at the receiving end.

The success of an MDC technique hinges on path diversity, which balances network load and reduces the probability of congestion. Typically, some amount of redundancy must be introduced at the source level in order that an acceptable reconstruction can be achieved from any of the descriptions, and such that reconstruction quality is enhanced with every description received. An issue of concern is the amount of redundancy introduced by the MDC representation with respect to a single-description coding, since there exists a tradeoff between this redundancy and the resulting distortion. Therefore, a great deal of effort has been spent on analyzing the performance achievable with MDC ever since its beginnings [162, 163] up until recently, for example, [164].

As an example of MDC, consider a wireless network in which a mobile receptor can benefit from multiple descriptions if they arrive independently, for example, on two neighboring access points. In this case, when moving between these two access points, the receiver might capture one or the other access point, and, in some cases, both. Another way to take advantage of MDC in a wireless environment is by splitting the transmission in frequency to form the two descriptions. For example, a laptop may be equipped with two wireless cards (e.g., 802.11a and g) with each wireless card receiving a different description. Depending on the dynamic changes in the number of clients in each network, one wireless card may become overloaded, and the corresponding description may not be transmitted. In wired networks, different descriptions can be routed to a receiver through different paths by incorporating this information into the packet header [165]. In this situation, the initial scenario of binary "on/off" channels might no longer be of interest. For example, in a typical CIF-format video sequence, one frame might be encoded into several packets. In such cases, the system should be designed to take into consideration individual or bursty packet losses rather than a whole description.

Practical approaches to MDC include scalar quantization [166–168], polyphase decompositions [169, 170], correlating transforms [171–177], and frame expansions [178–180]. We overview each of these strategies in the next sections below, first in the context of wavelet-based MDC for still images before turning attention to MDC for video to conclude this section.

3.1.1. Multiple-description scalar quantization

Multiple-description scalar quantization (MDSQ) [166] consists of encoding a memoryless stationary zero-mean source using a separate scalar quantizer for each description. The dictionaries of the scalar quantizers are determined from the minimization of the central distortion, subject to a maximal admissible distortion on the side distortions. Once the dictionaries are found, they must be indexed. In [166], two types of indexing are described: nested index assignment and linear index assignment. When one takes into account the rate on the two channels in addition to the distortion, the optimization problem is slightly different—in this case, the central distortion is minimized under rate as well as distortion constraints for the side decoders. Entropy coders follow the quantizers, and the system is called entropy-constrained MDSQ (ECMDSQ) [167]. An extension of the previous results to vectors was provided in [181–184] in the form of multiple-description lattice vector quantization.

In this special issue, the work "Scalable multiple-description image coding based on embedded quantization" by A. I. Gavrilescu et al. describes an embedded MDSQ which takes into account variations in the channel packet-loss rate to yield an adaptive bitrate allocation. This embedded MDSQ is applied to both still-image as well as video coders.

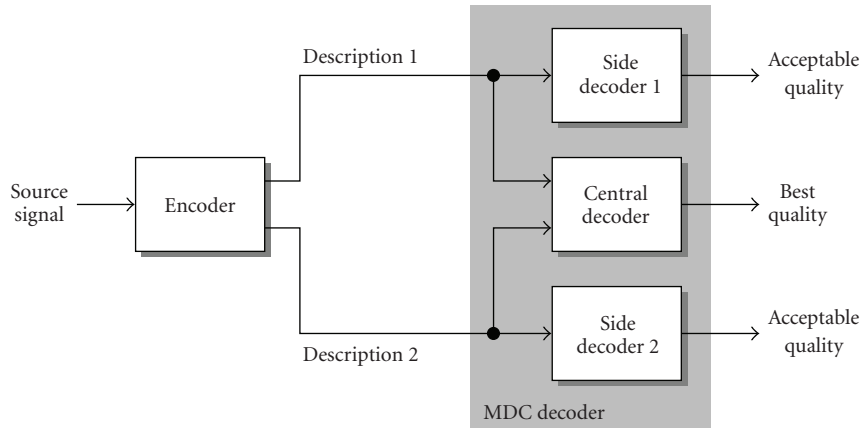

Figure 18: MDC with two descriptions.

3.1.2. Polyphase decompositions

A polyphase decomposition provides a straightforward and relatively simple approach to achieve MDC—one first splits the source samples into polyphase components (e.g., even and odd samples) and then encodes the polyphase components independently. Recall that the M polyphase components of a source $x[n]$ are the signals $y_1[n], y_2[n], \ldots, y_M[n]$ such that

$$y_i[n] = x[Mn + i], \quad n \in \mathbb{Z},\ i \in \{1, \ldots, M\}. \tag{4}$$

In the polyphase approach to MDC, each description consists of a single polyphase component, and, at the decoder side, the correlation between the components is exploited to recover any lost data.

This straightforward polyphase-based MDC strategy is refined slightly in [169] wherein, after polyphase decomposition, redundancy is introduced in each description by adding a low-rate version of the other polyphase components. As a consequence, each description involves a main polyphase component, encoded at high resolution, and several secondary polyphase components, encoded with less rate. The decoder simply merges the received polyphase components, and, if several versions of a given polyphase component are received, the decoder makes use of only the one encoded at the highest precision. For efficient coding, the polyphase signals must be decorrelated; if not, the decoder will be suboptimal, since it does not exploit the existing correlation. This system is therefore intended to be used after an initial source-coding step which consists of decorrelating the input data (e.g., a DWT or DCT).

For imagery, polyphase decompositions can be applied to different types of information in the image—pixels in the spatial domain, coefficients of a 2D DWT, or even zerotrees of wavelet coefficients (see Section 2.1.2). In this latter scheme, odd and even zerotrees are split into two descriptions and encoded as main and secondary components using SPIHT [169, 170].

It is useful to note that, whereas in most other MDC systems, redundancy between the descriptions is controlled only implicitly in the generation of the descriptions themselves, the polyphase-based MDC of [169] explicitly separates generation of the descriptions from the addition of redundancy; specifically, redundancy is controlled through the bitrate allocated to the secondary components. Thus, we find, in a certain sense, a separation principle between source coding (main quantization) and channel coding (added redundancy). While traditional source coding relies on a transform to reduce correlation between original-data (image) samples, MDC consists of the introduction of correlation in order to control redundancy in the transmitted bitstream. Below, we consider two types of correlation for the wavelet-based MDC of images—statistical correlation, through correlating transforms; and deterministic correlation, through projection onto frames.

In this special issue, the work "Multiple description coding with redundant expansions and application to image communications" by I. Radulovic and P. Frossard enters into the general polyphase MDC category. In the coder proposed in that work, a generic redundant dictionary is partitioned such that different, yet correlated, dictionary "atoms" are put into different descriptions.

3.1.3. Correlating transforms

A *multiple-description correlating transform* (MDCT) consists of transforming a block of N centered, independent Gaussian random variables into a block of N correlated variables. MDCT was introduced in [171, 172] for the case of $N = 2$ variables and generalized in [174, 175] to $N > 2$ variables. In [175], it was shown that performing quantization after a linear continuous-valued transform T led to a distortion significantly higher than when transform and quantization are performed in the reverse order. This is due to the fact that the quantization of $T\mathbf{x}$, $\mathbf{x} = [x_1 \ \ x_2]^T$, is equivalent to a trellis-coded quantization of vector $\mathbf{x}$ in a trellis whose cells are not square, which is suboptimal. The idea is therefore to look for an optimal discrete-valued transform $\widehat{T}(\mathbf{x})$ (to be applied to quantized vectors of the input source). For an equal probability of failure on the two channels, it is shown

in [175] that the optimal continuous-valued transform has the form

$$T = \begin{bmatrix} \alpha & (2\alpha)^{-1} \\ -\alpha & (2\alpha)^{-1} \end{bmatrix}, \tag{5}$$

where the parameter $\alpha \in [\sqrt{\sigma_2/2\sigma_1}, \infty)$ allows tuning the redundancy, ρ,

$$\rho = \frac{1}{2}\log\frac{\alpha^2\sigma_1^2 + \sigma_2^2/(4\alpha^2)}{\sigma_1\sigma_2}, \tag{6}$$

where σ_1^2 and σ_2^2 are the variances of the two sources. The discrete-valued $\hat{T}$ transform is then derived from (5) by factoring T into triangular matrices and then computing intermediate roundings of the triangular matrix factors. One can remark that, in the case that the two variances are equal, the side distortion is constant whatever the redundancy. In fact, this distortion is the same as that obtained when sending each source without transformation and estimating the missing source by the mean value in the case of a transmission failure. Moreover, the side distortion does not tend to zero when the rate tends to infinity. Finally, it was concluded in [175] that MDCT appears to be more efficient for low redundancies, while MDSQ, for example, is better at higher redundancies.

A generalization of the MDCT strategy was proposed in [176, 177]. There, an orthonormal two-band filterbank followed by different quantizers produces the correlation between the two descriptions. When one of the channels is off, for example the first one, the missing symbols transmitted on this channel are linearly estimated from the decoded symbols on the second channel. Since the size of the filters is not restricted, this framework is more general than that of the MDCT of [175], where the size of the transform is 2×2. Additionally, in [176, 177], the source is considered to be stationary Gaussian of power spectrum density (psd) $S(\omega)$ instead of independent and identically distributed as in [175]. Consequently, in [176, 177], rate-distortion theory for Gaussian processes (i.e., "reverse waterfilling" [185, 186]) is used to determine the optimal filters. Reverse waterfilling dictates that, for a sufficiently small distortion D, the minimum rate to transmit a Gaussian process with a psd of $S(\omega)$ is

$$R(D) = \frac{1}{2\pi}\int_{-\pi}^{\pi}\frac{1}{2}\log\frac{S(\omega)}{D}d\omega. \tag{7}$$

This formula is used to compute the transmission rate of the Gaussian variables on each channel, supposing that the entropy coding achieves its theoretical limit. Moreover, an optimal allocation among the channels is assumed; consequently, the two descriptions $y_i[n]$, $i \in \{1, 2\}$, are transmitted at the rates

$$R_i(D_0) = \frac{1}{2\pi}\int_{-\pi}^{\pi}\frac{1}{2}\log\frac{Y_i(\omega)}{D_0}d\omega, \tag{8}$$

where $Y_i(\omega)$ is the psd of $y_i[n]$, and D_0 is the central distortion. The redundancy is then

$$\rho(D_0) = \frac{1}{2}(R_1(D_0) + R_2(D_0)) - \frac{1}{2\pi}\int_{-\pi}^{\pi}\frac{1}{2}\log\frac{S(\omega)}{D_0}d\omega, \tag{9}$$

the second term corresponding to the rate-distortion curve of the source $x[n]$ with psd $S(\omega)$. In case of failure on channel 1, $y_1[n]$ is estimated by Wiener filtering as $Y_{21}(\omega)/Y_2(\omega)$, where $Y_{21}(\omega)$ is the cross-psd of $y_1[n]$ and $y_2[n]$. One can then compute the side distortions D_1 and D_2 which are approximately equal to the estimation errors of $y_1[n]$ and $y_2[n]$ by the Wiener filter. The frequency responses of the optimal filters, $H_1(\omega)$ and $H_2(\omega)$, are then the solution of

$$\min_{H_1(\omega),H_2(\omega)}\frac{1}{2}(D_1 + D_2) + \lambda\rho(D_0), \tag{10}$$

with the central distortion fixed. The Lagrangian parameter λ also allows adjusting the redundancy and thus the balance between central and side distortions. The following conclusions of this study are of interest.

(1) When $\lambda \to \infty$, one simply tries to minimize the redundancy ρ. In this case, we arrive at classical source-coding results, with the optimal filters producing decorrelated variables $y_1[n]$ and $y_2[n]$. The filterbank is, in this case, a Karhunen-Loève transform.
(2) When $\lambda = 0$, the redundancy is not taken into account, and one minimizes only the side distortions. The optimal filterbank then corresponds to a polyphase decomposition, and the correlation between $y_1[n]$ and $y_2[n]$ is maximal.
(3) If the source is independent and identically distributed by blocks of 2 (i.e., vectors of two successive samples are Gaussian, independent, and identically distributed), the optimal filters will be FIR of length 2, and we arrive at the MDCT of [175]; this result was also shown in [187].

The work in [176, 177] also provides optimal filters for an AR(1) process and compares to classical orthonormal wavelet transforms (Haar, Daubechies, Coifman).

3.1.4. *Correlation through frames*

A frame is a family of vectors generating a Hilbert space; contrary to a decomposition in a basis, frame decompositions often lead to redundant coefficients. Moreover, the correlation in such a redundant decomposition is deterministic, since, for a vector space of dimension N, N coefficients suffice to reconstruct the original signal. The redundancy permits, on the one hand, reduction of quantization noise [188], and, on the other hand, recovery after channel errors. In fact, it was shown that uniform tight frames are optimal in the case of erasures [179].

The difference between error resilience via frames and that obtained through a traditional error-correcting code comes from the placement of quantization—in the frame-based approach, redundancy is added before quantization (by the frame-based transform), whereas, in channel coding, redundancy is added after quantization. Even though it is difficult to perform a theoretical comparison that deduces the superiority of one approach with respect to the other, a numerical comparison of the two schemes is presented in [178] for a Gaussian source of dimension $N = 4$, comparing a harmonic frame of dimension $M = 5$ to a $(5, 4)$ block

code. From this comparison, the advantage of frames occurs at high bitrate and for a very low, or very high, packet-loss rate. Otherwise, error-correcting codes are better. However, when there are no packet losses, the redundancy added by the channel code cannot be exploited, whereas frame-based redundancy can still be used by the decoder to reduce quantization noise.

3.1.5. MDC for video

Several directions have been investigated for video using MDC. In [189–192], the proposed schemes are largely deployed in the spatial domain within hybrid video coders such as MPEG and H.264/AVC; a thorough survey on MDC for such hybrid coders can be found in [193].

On the other hand, only a few works investigate MDC schemes that introduce source redundancy in the temporal domain, although this approach has shown some promise. In [194], a balanced interframe MDC was proposed starting from the popular DPCM technique. In [195], the reported MDC scheme consists of temporal subsampling of the coded error samples by a factor of 2 so as to obtain two threads at the encoder which are further independently encoded using prediction loops that mimic the decoders (i.e., two side prediction loops and a central prediction loop).

MDC has also been applied to MCTF-based video coding (see Section 2.2.2); existing work for $t + 2D$ video codecs with temporal redundancy addresses 3-band filter banks [196, 197]. Another direction for wavelet-based MDC video uses the polyphase approach in the temporal or spatiotemporal domain of coefficients [198–200].

In this special issue, the work "A motion-compensated overcomplete temporal decomposition for multiple description scalable video coding" by C. Tillier et al. focuses on a two-description coding scheme for scalable video, wherein temporal and spatial scalability follow from a classical dyadic subband transform. The correlation between the two descriptions is introduced in the temporal domain by exploiting an oversampled MCTF. An important feature of the proposed scheme is its reduced redundancy, which is achieved by an additional subsampling of the resulting temporal details. The remaining detail coefficients are then distributed in a balanced manner between the two descriptions, along with the nondecimated approximation coefficients. The global redundancy is thus tuned by the number of temporal decomposition levels.

3.2. Joint source-channel coding

Shannon's separability theorem [201] states that if the minimum achievable source-coding rate of a given source is below the capacity of a channel, then that source can be reliably transmitted through the channel. In addition, it states that the source and channel encoders can be separated in such a way that the source-coding rate reduction takes place in the source encoder, while the protection against channel errors occurs separately in the channel encoder—that is, source and channel coding can be treated separately without any loss of performance for the overall system. Such a concatenation of a source coder followed by a channel coder which are separately optimized is a *tandem* communication scheme. However, Shannon's separation theorem, and thus tandem communication, is valid only for blocks of source and channel symbols sufficiently long and for encoders and decoders of arbitrarily large complexity.

In practical situations, there are limitations on both system complexity and block length which call into question the validity of separate design. In recent decades, alternative approaches consisting of combining source and channel coding have arisen. The objective is to include both source- and channel-coding modules in the same processing block in order to reduce the complexity of the overall system while simultaneously increasing the system performance in a nonideal, real-world setting. Typically, efforts toward such *joint source-channel coding* have focused on either designing channel coding with respect to a fixed source—*source-optimized channel coding*—or on designing source coding with respect to a fixed channel—*channel-optimized source coding*. Below, we overview both strategies as applied to wavelet-based image and video source coders.

3.2.1. Source-optimized channel coding

In source-optimized channel coding, the source code is first designed and optimized for a noiseless channel. A channel code is then designed for this fixed source code so as to minimize end-to-end distortion over a given channel (typically a binary symmetric channel (BSC), an additive white Gaussian noise (AWGN) channel with a given modulation, or a time-varying channel).

For example, [202] considers transmission of a video sequence over fading channels. A 3D spatiotemporal subband decomposition followed by vector quantization (VQ) of the subband coefficients forms the source coder, while the VQ indexes of each coded subband are interleaved and protected using *rate-compatible punctured convolutional* (RCPC) codes [203]. The source-coding and channel-coding rates are jointly chosen on a subband-by-subband basis to minimize the total end-to-end mean distortion. Interleaving facilitates the analytical computation of the channel-induced distortion by making the equivalent channel memoryless, and the optimal allocation of source- and channel-coding rates is formulated as a constrained optimization problem.

In [204, 205], 3D subband coding using multirate quantization and bit sensitivity over noisy channels is considered for video. An analytical expression for the end-to-end transmission distortion is found for the case of a scalable subband coding scheme protected with RCPC codes. The source coder consists of 3D spatiotemporal subbands which are successively refined via layered quantization and finally coded by a conditional arithmetic coding. In the case of channel errors, *unequal error protection* (UEP) of the source bits is applied using RCPC codes such that source bits deemed more important to the end-to-end quality are given more protection. The problem of optimal partitioning of source- and channel-coding bits is based on two assumptions. First, all bits within

the same quantization layer must receive the same level of protection, and second, higher quantization layers never receive more protection than lower layers. These constraints are formulated as

$$\min_{\mathbf{n},\mathbf{m}} D = \min_{\mathbf{n},\mathbf{m}} \sum_k d_k(n_k, m_k) \tag{11}$$

subject to

$$\begin{aligned} \sum_k n_k &\le R_s, \\ \sum_k m_k &\le B - R_s = R_c, \end{aligned} \tag{12}$$

where $\mathbf{m} = [m_1 \ \cdots \ m_K]$ is the distribution vector of channel bits used to protect $\mathbf{n} = [n_1 \ \cdots \ n_K]$ source bits in subbands $k = 1, \ldots, K$; $d_k(n_k, m_k)$ is the distortion for subband k; B is the total bit budget; and R_s and R_c are the target source and channel rates, respectively. Thus, the corresponding unconstrained Lagrangian problem is

$$\min_{\mathbf{m},\mathbf{n}} \sum_k \left(d_k(n_k, m_k) + \lambda n_k + \mu m_k \right). \tag{13}$$

If there exist multipliers λ and μ such that the source- and channel-rate budgets are satisfied with equality, then the optimal solution to the Lagrangian problem is also the optimal solution to the original problem. In [205], an extended analysis of the estimation of these Lagrange multipliers is presented. The algorithm is based on [206] with an extension to two Lagrangian parameters. It is shown that, when the error probability of the channel increases, the total number of quantization layers selected decreases. In addition, in low-noise channel conditions, the high-frequency layers are dropped largely due to the low error sensitivity of the high-frequency components. On the other hand, in high-noise channel conditions, the number of layers of low-frequency subbands is reduced. Finally, it is shown that the above optimized codec with RCPC-based UEP outperforms the case wherein *equal error protection* (EEP) is used (i.e., all source bits receive the same level of protection).

In [207], a method for optimal rate allocation for standard video encoders is presented. This rate allocation is based upon an assumption of dependence between the video frames, and, to limit the complexity of this otherwise difficult problem, models are proposed for the operational distortion-rate characteristics as well as the channel-code bit-error rate (BER) as a function of the available bandwidth. The compressed video is channel-coded using rate-compatible punctured systematic recursive convolutional (RCPSRC) codes [208]. The focus is on rate allocation at the frame level, and a single quantization parameter per frame is selected. Specifically, $\mathbf{q} = [q_1 \ \cdots \ q_K]$ is the vector of quantization parameters for a K-frame group of pictures (GOP) where $q_k \in \{1, 2, \ldots, 31\}$ is the quantization parameter for frame k. Similarly, the channel encoder assigns a selected channel-coding rate r_k to each frame with $\mathbf{r} = [r_1 \ \cdots \ r_K]$ being the vector of channel-code rates for the K-frame sequence. The general minimization problem is then, given a set $\mathcal{Q}$ of admissible quantizers and a set $\mathcal{R}$ of admissible channel-coding rates, find $\mathbf{q}^*$ (with each $q_k^* \in \mathcal{Q}$) and $\mathbf{r}^*$ (with each $r_k^* \in \mathcal{R}$) such that

$$(\mathbf{q}^*, \mathbf{r}^*) = \arg\min_{\mathbf{q},\mathbf{r}} D(\mathbf{q}, \mathbf{r}) \tag{14}$$

subject to

$$\frac{1}{K} \sum_k \frac{R_s^{(k)}(q_k)}{r_k} \le \frac{1}{K} R, \tag{15}$$

where $D(\mathbf{q}, \mathbf{r})$ is the average K-frame sequence distortion, R is the overall rate constraint, and $R_s^{(k)}(q_k)$ is the source-rate function for frame k. In order to perform an optimal rate allocation through the above minimization, a model for RCPSRC codes is proposed. In general, the results show that more rate should be allocated to earlier frames in a sequence than to later frames, and that, for a fixed source-coding rate, there is a significant advantage to a UEP strategy that allows variable channel-coding rates between frames in a sequence.

In [209], the 3D-SPIHT video coder of [22, 23] is cascaded with RCPC codes applied in combination with an *automatic repeat request* (ARQ) for transmission over a BSC. The 3D-SPIHT bitstream is partitioned into blocks of equal length with each block receiving parity bits from a cyclic redundancy code (CRC) before being passed into the RCPC code. At the receiver side, a Viterbi decoder is employed, and, if the decoder fails to decode the received block within a certain trellis depth, a negative ARQ acknowledgment is sent back to the transmitter thereby requesting re-transmission of the same block. We note that the use of ARQ results in delay that may be incompatible with the needs of real-time communications and requires the additional bandwidth of the feedback channel.

In [210], the 3D wavelet coefficients are divided into several groups according to their spatial and temporal relationships and then each group is encoded independently using 3D-SPIHT. The channel-coding procedure of [209] is employed without ARQ. By coding the wavelet coefficients into multiple independent bitstreams, any single bit error affects only one of these streams, while the others are received unaffected. Decoding of a bitstream simply stops if a certain trellis depth is reached without successful decoding of a received packet, and the decoding procedure continues until either the final packet has arrived or a decoding failure has occurred in all bitstreams.

In [211], UEP of 3D-SPIHT is proposed with the channel coding of [209] applied on unequally long segments of the bitstream. Lower RCPC code rates are used for the more sensitive, significant subblocks to provide better error protection, while larger RCPC code rates are used for insensitive, insignificant subblocks. It is observed that, when the noise exceeds a certain level for a fixed RCPC code rate, the performance of an EEP scheme will deteriorate immediately, while the proposed UEP strategy provides a better tradeoff between rate-distortion performance and error resilience.

In this special issue, the work "Progressive image transmission based on joint source-channel decoding using adaptive sum-product algorithm" by W. Liu and D. G. Daut

designs an iterative procedure for the joint decoding of *low-density parity-check* (LDPC) codes [212, 213] and a JPEG2000 bitstream. The proposed method exploits error-resilience information from the JPEG2000 source code to drive the channel decoder. During each decoder iteration, a tentative guess at the decoded channel bits is provided to the source decoder, with the positions of error-free bits as determined by the source decoder being fed back to the channel decoder. Experimental results reveal that the joint decoder reduces the number of decoder iterations and improves distortion performance as compared to a similar system that is not source-controlled.

3.2.2. Channel-optimized source coding

In channel-optimized source coding, the source code is designed by minimizing a distortion criterion which includes the effect of channel errors on the channel code. Typically this is accomplished by designing the codebook for the quantizer within the source coder for the specific channel in question.

An early attempt in this area is [214] wherein, instead of considering the quantizer and the channel encoder separately, the focus is on the design of an encoder function that maps the output of the source-coder quantizer to the channel input. For a fixed decoder, necessary conditions for the optimality of the encoder function are derived. Subsequently, necessary conditions for the optimality of the decoder are derived for a fixed encoder function. The resulting set of conditions are merely necessary, and not sufficient, for overall system optimality; consequently, the final solution obtained is only locally optimal.

In this special issue, in this category, "Joint source-channel coding for wavelet-based scalable video transmission using an adaptive turbo code" by N. Ramzan et al. proposes a scalable, wavelet-based video coder which is jointly optimized with a turbo encoder providing UEP for the subbands. The end-to-end distortion taking into account channel rate, turbo-code packet size, as well as the interleaver is minimized at given channel conditions by an iterative procedure. Also in this special issue is "Content-adaptive packetization and streaming of wavelet video over IP networks" by C.-P. Ho and C.-J. Tsai which proposes a 3D video wavelet codec followed by forward error correction (FEC) for UEP with the focus being on the content-adaptive packetization for video streaming over IP networks. At a given packet-loss rate, the video distortion resulting from packet loss is translated into source distortion, thus yielding the best FEC protection level. The run-time packet-loss rate that is fed back from the receiver also enters into the optimization algorithm for choosing the FEC protection level. Finally, a similar approach in a different context is presented in "Energy-efficient transmission of wavelet-based images in wireless sensor networks" by V. Lecuire et al. in this special issue. In this work, image quality and energy consumption are jointly optimized over a wireless sensor network. The image encoder, which uses a 2D DWT, is adapted according to the state of the network (global energy dissipated in all the nodes between the transmitter and receiver) so as to send a greater or lesser number of resolution levels. The model for energy consumption involves the image-transmission energy, the radio-transceiver consumption, and the energy required to perform the 2D DWT. Despite the fact that the optimization criterion employed is not identical to that of classical joint source-channel coding, the source encoding and packetization are optimized to follow the channel (energy) conditions in much the same way as the other channel-optimized source-coding schemes surveyed here.

4. CONCLUSION

In this paper, we have surveyed a number of salient examples of the use of wavelets in source coding, communications, and networking, and the papers that follow in this special issue delve into greater depth in topics of recent interest in these areas. We have, however, by no means exhaustively covered all the image and video applications that have been impacted by wavelets and wavelet theory. Indeed, we anticipate that wavelets will remain firmly entrenched in widespread applications in image and video processing for some time to come.

ACKNOWLEDGMENTS

This work was funded in part by the French Agence Nationale de la Recherche (ANR) under Grant no. ANR-05-RNRT-019 (DIVINE project), by the French Centre National de la Recherche Scientifique (CNRS), and by the US National Science Foundation (NSF) under Grant no. CCR-0310864. The authors thank S. Cui, J. B. Boettcher, G. Feideropoulou, L. Hua, G. Pau, J. T. Rucker, C. Tillier, and Y. Wang for numerous and sundry contributions to the work leading up to this manuscript.

REFERENCES

[1] J. E. Fowler, "Embedded wavelet-based image compression: state of the art (Eingebettete wavelet-basierte bildkompression: stand der technik)," *Information Technology*, vol. 45, no. 5, pp. 256–262, 2003.

[2] J. E. Fowler and J. T. Rucker, "3D wavelet-based compression of hyperspectral imagery," in *Hyperspectral Data Exploitation: Theory and Applications*, C.-I. Chang, Ed., chapter 14, pp. 379–407, John Wiley & Sons, Hoboken, NJ, USA, 2007.

[3] J. T. Rucker and J. E. Fowler, "Shape-adaptive embedded coding of ocean-temperature imagery," in *Proceedings of the 40th Asilomar Conference on Signals, Systems, and Computers*, pp. 1887–1891, Pacific Grove, Calif, USA, October 2006.

[4] K. Ramchandran and M. Vetterli, "Best wavelet packet bases in a rate-distortion sense," *IEEE Transactions on Image Processing*, vol. 2, no. 2, pp. 160–175, 1993.

[5] J. N. Bradley, C. M. Brislawn, and T. Hopper, "FBI wavelet/scalar quantization standard for gray-scale fingerprint image compression," in *Visual Information Processing II*, vol. 1961 of *Proceedings of SPIE*, pp. 293–304, Orlando, Fla, USA, April 1993.

[6] B. Penna, T. Tillo, E. Magli, and G. Olmo, "Progressive 3-D coding of hyperspectral images based on JPEG 2000," *IEEE Geoscience and Remote Sensing Letters*, vol. 3, no. 1, pp. 125–129, 2006.

[7] E. Christophe, C. Mailhes, and P. Duhamel, "Best anisotropic 3-D wavelet decomposition in a rate-distortion sense," in *Proceedings of IEEE International Conference on Acoustics, Speech, and Signal Processing (ICASSP '06)*, vol. 2, pp. 17–20, Toulouse, France, May 2006.

[8] J. M. Shapiro, "Embedded image coding using zerotrees of wavelet coefficients," *IEEE Transactions on Signal Processing*, vol. 41, no. 12, pp. 3445–3462, 1993.

[9] A. Said and W. A. Pearlman, "A new, fast, and efficient image codec based on set partitioning in hierarchical trees," *IEEE Transactions on Circuits and Systems for Video Technology*, vol. 6, no. 3, pp. 243–250, 1996.

[10] A. Islam and W. A. Pearlman, "Embedded and efficient low-complexity hierarchical image coder," in *Visual Communications and Image Processing*, K. Aizawa, R. L. Stevenson, and Y.-Q. Zhang, Eds., vol. 3653 of *Proceedings of SPIE*, pp. 294–305, San Jose, Calif, USA, January 1999.

[11] W. A. Pearlman, A. Islam, N. Nagaraj, and A. Said, "Efficient, low-complexity image coding with a set-partitioning embedded block coder," *IEEE Transactions on Circuits and Systems for Video Technology*, vol. 14, no. 11, pp. 1219–1235, 2004.

[12] J. E. Fowler, "Shape-adaptive coding using binary set splitting with k-d trees," in *Proceedings of IEEE International Conference on Image Processing (ICIP '04)*, vol. 2, pp. 1301–1304, Singapore, October 2004.

[13] "Information Technology—JPEG 2000 Image Coding System—Part 1: Core Coding System," ISO/IEC 15444-1, 2000.

[14] M. Antonini, M. Barlaud, P. Mathieu, and I. Daubechies, "Image coding using wavelet transform," *IEEE Transactions of Image Processing*, vol. 1, no. 2, pp. 205–220, 1992.

[15] D. Le Gall and A. Tabatabai, "Sub-band coding of digital images using symmetric short kernel filters and arithmetic coding techniques," in *Proceedings of IEEE International Conference on Acoustics, Speech, and Signal Processing (ICASSP '88)*, pp. 761–764, New York, NY, USA, April 1988.

[16] J. D. Villasenor, B. Belzer, and J. Liao, "Wavelet filter evaluation for image compression," *IEEE Transactions on Image Processing*, vol. 4, no. 8, pp. 1053–1060, 1995.

[17] A. R. Calderbank, I. Daubechies, W. Sweldens, and B.-L. Yeo, "Lossless image compression using integer to integer wavelet transforms," in *Proceedings of IEEE International Conference on Image Processing (ICIP '97)*, vol. 1, pp. 596–599, Santa Barbara, Calif, USA, October 1997.

[18] A. R. Calderbank, I. Daubechies, W. Sweldens, and B.-L. Yeo, "Wavelet transforms that map integers to integers," *Applied and Computational Harmonic Analysis*, vol. 5, no. 3, pp. 332–369, 1998.

[19] "Information Technology—JPEG 2000 Image Coding System—Part 2: Extensions," ISO/IEC 15444-2, 2004.

[20] Y. Chen and W. A. Pearlman, "Three-dimensional subband coding of video using the zero-tree method," in *Visual Communications and Image Processing*, R. Ansari and M. J. T. Smith, Eds., vol. 2727 of *Proceedings of SPIE*, pp. 1302–1312, Orlando, Fla, USA, March 1996.

[21] P. Campisi, M. Gentile, and A. Neri, "Three dimensional wavelet based approach for a scalable video conference system," in *Proceedings of IEEE International Conference on Image Processing (ICIP '99)*, vol. 3, pp. 802–806, Kobe, Japan, October 1999.

[22] B.-J. Kim and W. A. Pearlman, "An embedded wavelet video coder using three-dimensional set partitioning in hierarchical trees (SPIHT)," in *Proceedings of Data Compression Conference (DCC '97)*, J. A. Storer and M. Cohn, Eds., pp. 251–260, Snowbird, Utah, USA, March 1997.

[23] B.-J. Kim, Z. Xiong, and W. A. Pearlman, "Low bit-rate scalable video coding with 3-D set partitioning in hierarchical trees (3-D SPIHT)," *IEEE Transactions on Circuits and Systems for Video Technology*, vol. 10, no. 8, pp. 1374–1387, 2000.

[24] P. L. Dragotti, G. Poggi, and A. R. P. Ragozini, "Compression of multispectral images by three-dimensional SPIHT algorithm," *IEEE Transactions on Geoscience and Remote Sensing*, vol. 38, no. 1, pp. 416–428, 2000.

[25] C. He, J. Dong, Y. F. Zheng, and Z. Gao, "Optimal 3-D coefficient tree structure for 3-D wavelet video coding," *IEEE Transactions on Circuits and Systems for Video Technology*, vol. 13, no. 10, pp. 961–972, 2003.

[26] S. Cho and W. A. Pearlman, "Error resilient video coding with improved 3-D SPIHT and error concealment," in *Image and Video Communications and Processing*, B. Vasudev, T. R. Hsing, A. G. Tescher, and T. Ebrahimi, Eds., vol. 5022 of *Proceedings of SPIE*, pp. 125–136, Santa Clara, Calif, USA, January 2003.

[27] X. Tang, S. Cho, and W. A. Pearlman, "3D set partitioning coding methods in hyperspectral image compression," in *Proceedings of IEEE International Conference on Image Processing (ICIP '03)*, vol. 2, pp. 239–242, Barcelona, Spain, September 2003.

[28] M. W. Marcellin and A. Bilgin, "Quantifying the parent-child coding gain in zero-tree-based coders," *IEEE Signal Processing Letters*, vol. 8, no. 3, pp. 67–69, 2001.

[29] X. Tang, W. A. Pearlman, and J. W. Modestino, "Hyperspectral image compression using three-dimensional wavelet coding," in *Image and Video Communications and Processing*, B. Vasudev, T. R. Hsing, A. G. Tescher, and T. Ebrahimi, Eds., vol. 5022 of *Proceedings of SPIE*, pp. 1037–1047, Santa Clara, Calif, USA, January 2003.

[30] X. Tang and W. A. Pearlman, "Three-dimensional wavelet-based compression of hyperspectral images," in *Hyperspectral Data Compression*, G. Motta, F. Rizzo, and J. A. Storer, Eds., chapter 10, pp. 273–308, Kluwer Academic Publishers, Norwell, Mass, USA, 2006.

[31] J. T. Rucker and J. E. Fowler, "Coding of ocean-temperature volumes using binary set splitting with k-d trees," in *Proceedings of IEEE International Geoscience and Remote Sensing Symposium (IGARSS '04)*, vol. 1, pp. 289–292, Anchorage, Alaska, USA, September 2004.

[32] D. S. Taubman and M. W. Marcellin, *JPEG2000: Image Compression Fundamentals, Standards and Practice*, Kluwer Academic Publishers, Boston, Mass, USA, 2002.

[33] M. Rabbani and R. Joshi, "An overview of the JPEG 2000 still image compression standard," *Signal Processing: Image Communication*, vol. 17, no. 1, pp. 3–48, 2002.

[34] A. Skodras, C. Christopoulos, and T. Ebrahimi, "The JPEG 2000 still image compression standard," *IEEE Signal Processing Magazine*, vol. 18, no. 5, pp. 36–58, 2001.

[35] D. Taubman, "High performance scalable image compression with EBCOT," *IEEE Transactions on Image Processing*, vol. 9, no. 7, pp. 1158–1170, 2000.

[36] J. T. Rucker, J. E. Fowler, and N. H. Younan, "JPEG2000 coding strategies for hyperspectral data," in *Proceedings of IEEE International Geoscience and Remote Sensing Symposium (IGARSS '05)*, vol. 1, pp. 128–131, Seoul, South Korea, July 2005.

[37] P. Schelkens, J. Barbarien, and J. Cornelis, "Compression of volumetric medical data based on cube-splitting," in *Applications of Digital Image Processing XXIII*, vol. 4115 of *Proceedings of SPIE*, pp. 91–101, San Diego, Calif, USA, July 2000.

[38] "Digital Compression and Coding of Continuous-Tone Still Image—Part 1: requirements and guidelines,," ISO/IEC 10918-1, 1991.

[39] W. B. Pennebaker and J. L. Mitchell, *JPEG Still Image Compression Standard*, Kluwer Academic Publishers, Boston, Mass, USA, 1993.

[40] J. E. Fowler, "QccPack: an open-source software library for quantization, compression, and coding," in *Applications of Digital Image Processing XXIII*, A. G. Tescher, Ed., vol. 4115 of *Proceedings of SPIE*, pp. 294–301, San Diego, Calif, USA, July-August 2000.

[41] "Information Technology—Coding of Audio-Visual Objects—Part 2: Visual," ISO/IEC 14496-2, 1999, MPEG-4 Coding Standard.

[42] S. Li and W. Li, "Shape-adaptive discrete wavelet transforms for arbitrarily shaped visual object coding," *IEEE Transactions on Circuits and Systems for Video Technology*, vol. 10, no. 5, pp. 725–743, 2000.

[43] G. Minami, Z. Xiong, A. Wang, and S. Mehrotra, "3-D wavelet coding of video with arbitrary regions of support," *IEEE Transactions on Circuits and Systems for Video Technology*, vol. 11, no. 9, pp. 1063–1068, 2001.

[44] Z. Lu and W. A. Pearlman, "Wavelet coding of video object by object-based SPECK algorithm," in *Proceedings of the 22nd Picture Coding Symposium (PCS '01)*, pp. 413–416, Seoul, South Korea, April 2001.

[45] J. E. Fowler, "Shape-adaptive tarp coding," in *Proceedings of IEEE International Conference on Image Processing (ICIP '03)*, vol. 1, pp. 621–624, Barcelona, Spain, September 2003.

[46] G. Ziegler, H. P. A. Lensch, N. Ahmed, M. Magnor, and H.-P. Seidel, "Multi-video compression in texture space," in *Proceedings of IEEE International Conference on Image Processing (ICIP '04)*, vol. 4, pp. 2467–2470, Singapore, October 2004.

[47] H. Wang, G. M. Schuster, and A. K. Katsaggelos, "Rate-distortion optimal bit allocation for object-based video coding," *IEEE Transactions on Circuits and Systems for Video Technology*, vol. 15, no. 9, pp. 1113–1123, 2005.

[48] J. E. Fowler and D. N. Fox, "Embedded wavelet-based coding of three-dimensional oceanographic images with land masses," *IEEE Transactions on Geoscience and Remote Sensing*, vol. 39, no. 2, pp. 284–290, 2001.

[49] J. E. Fowler and D. N. Fox, "Wavelet-based coding of three-dimensional oceanographic images around land masses," in *Proceedings of IEEE International Conference on Image Processing (ICIP '00)*, vol. 2, pp. 431–434, Vancouver, BC, Canada, September 2000.

[50] M. Cagnazzo, G. Poggi, L. Verdoliva, and A. Zinicola, "Region-oriented compression of multispectral images by shape-adaptive wavelet transform and SPIHT," in *Proceedings of IEEE International Conference on Image Processing (ICIP '04)*, vol. 4, pp. 2459–2462, Singapore, October 2004.

[51] M. Cagnazzo, G. Poggi, and L. Verdoliva, "A comparison of flat and object-based transform coding techniques for the compression of multispectral images," in *Proceedings of IEEE International Conference on Image Processing (ICIP '05)*, vol. 1, pp. 657–660, Genova, Italy, September 2005.

[52] M. Penedo, W. A. Pearlman, P. G. Tahoces, M. Souto, and J. J. Vidal, "Region-based wavelet coding methods for digital mammography," *IEEE Transactions on Medical Imaging*, vol. 22, no. 10, pp. 1288–1296, 2003.

[53] J. Hua, Z. Xiong, Q. Wu, and K. R. Castleman, "Fast segmentation and lossy-to-lossless compression of DNA microarray images," in *Proceedings of the Workshop on Genomic Signal Processing and Statistics (GENSIPS ' 02)*, Raleigh, NC, USA, October 2002.

[54] Z. Liu, J. Hua, Z. Xiong, Q. Wu, and K. R. Castleman, "Lossy-to-lossless ROI coding of chromosome images using modified SPIHT and EBCOT," in *Proceedings of IEEE International Symposium on Biomedical Imaging (ISBI '02)*, pp. 317–320, Washington, DC, USA, July 2002.

[55] J. Hua, Z. Liu, Z. Xiong, Q. Wu, and K. R. Castleman, "Microarray BASICA: background adjustment, segmentation, image compression and analysis of microarray images," *EURASIP Journal on Applied Signal Processing*, vol. 2004, no. 1, pp. 92–107, 2004.

[56] H.-W. Park and H.-S. Kim, "Motion estimation using low-band-shift method for wavelet-based moving-picture coding," *IEEE Transactions on Image Processing*, vol. 9, no. 4, pp. 577–587, 2000.

[57] P. Chen and J. W. Woods, "Bidirectional MC-EZBC with lifting implementation," *IEEE Transactions on Circuits and Systems for Video Technology*, vol. 14, no. 10, pp. 1183–1194, 2004.

[58] B. Wang, Y. Wang, I. Selesnick, and A. Vetro, "Video coding using 3-D dual-tree discrete wavelet transforms," in *Proceedings of IEEE International Conference on Acoustics, Speech, and Signal Processing (ICASSP '05)*, vol. 2, pp. 61–64, Philadelphia, Pa, USA, March 2005.

[59] "Information Technology—Generic Coding of Moving Pictures and Associated Audio Information: Video," ISO/IEC 13818-2, MPEG-2 Video Coding Standard, 1995.

[60] "Advanced Video Coding for Generic Audiovisual Services," ITU-T, ITU-T Recommendation H.264, May 2003.

[61] S. A. Martucci, I. Sodagar, T. Chiang, and Y.-Q. Zhang, "A zerotree wavelet video coder," *IEEE Transactions on Circuits and Systems for Video Technology*, vol. 7, no. 1, pp. 109–118, 1997.

[62] G. van der Auwera, A. Munteanu, G. Lafruit, and J. Cornelis, "Video coding based on motion estimation in the wavelet detail images," in *Proceedings of IEEE International Conference on Acoustics, Speech, and Signal Processing (ICASSP '98)*, vol. 5, pp. 2801–2804, Seattle, Wash, USA, May 1998.

[63] Y.-Q. Zhang and S. Zafar, "Motion-compensated wavelet transform coding for color video compression," *IEEE Transactions on Circuits and Systems for Video Technology*, vol. 2, no. 3, pp. 285–296, 1992.

[64] F. Dufaux, I. Moccagatta, B. Rouchouze, T. Ebrahimi, and M. Kunt, "Motion-compensated generic coding of video based on a multiresolution data structure," *Optical Engineering*, vol. 32, no. 7, pp. 1559–1570, 1993.

[65] C. Cafforio, C. Guaragnella, F. Bellifemine, A. Chimienti, and R. Picco, "Motion compensation and multiresolution coding," *Signal Processing: Image Communication*, vol. 6, no. 2, pp. 123–142, 1994.

[66] R. C. Zaciu and F. Bellifemine, "A compression method for image sequences," in *Proceedings of IEEE International Conference on Consumer Electronics (ICCE '94)*, M. A. Isnardi and W. F. Wedam, Eds., pp. 230–231, Chicago, Ill, USA, June 1994.

[67] R. C. Zaciu, C. Lamba, C. Burlacu, and G. Nicula, "Image compression using an overcomplete discrete wavelet transform," *IEEE Transactions on Consumer Electronics*, vol. 42, no. 3, pp. 800–807, 1996.

[68] C. S. Burrus, R. A. Gopinath, and H. Guo, *Introduction to Wavelets and Wavelet Transforms: A Primer*, Prentice Hall, Upper Saddle River, NJ, USA, 1998.

[69] P. Dutilleux, "An implementation of the "algorithme à trous" to compute the wavelet transform," in *Wavelets: Time-Frequency Methods and Phase Space*, J.-M. Combes, A. Grossmann, and P. Tchamitchian, Eds., pp. 298–304, Springer, Berlin, Germany, 1989, Proceedings of the International Conference, Marseille, France, December 1987.

[70] M. Holschneider, R. Kronland-Martinet, J. Morlet, and P. Tchamitchian, "A real-time algorithm for signal analysis with the help of the wavelet transform," in *Wavelets: Time-Frequency Methods and Phase Space*, J.-M. Combes, A. Grossmann, and P. Tchamitchian, Eds., pp. 286–297, Springer, Berlin, Germany, 1989, Proceedings of the International Conference, Marseille, France, December 1987.

[71] M. J. Shensa, "The discrete wavelet transform: wedding the à trous and Mallat algorithms," *IEEE Transactions on Signal Processing*, vol. 40, no. 10, pp. 2464–2482, 1992.

[72] H. S. Kim and H. W. Park, "Wavelet-based moving-picture coding using shift-invariant motion estimation in wavelet domain," *Signal Processing: Image Communication*, vol. 16, no. 7, pp. 669–679, 2001.

[73] Y. Andreopoulos, A. Munteanu, G. van der Auwera, P. Schelkens, and J. Cornelius, "Wavelet-based fully-scalable video coding with in-band prediction," in *Proceedings of the 3rd IEEE Benelux Signal Processing Symposium (SPS '02)*, pp. 217–220, Leuven, Belgium, March 2002.

[74] X. Li and L. Kerofsky, "High performance resolution scalable video coding via all-phase motion compensated prediction of wavelet coefficients," in *Visual Communications and Image Processing*, C.-C. J. Kuo, Ed., vol. 4671 of *Proceedings of SPIE*, pp. 1080–1090, San Jose, Calif, USA, January 2002.

[75] X. Li, L. Kerofsky, and S. Lei, "All-phase motion compensated prediction in the wavelet domain for high performance video coding," in *Proceedigs of IEEE International Conference on Image Processing (ICIP '01)*, vol. 3, pp. 538–541, Thessaloniki, Greece, October 2001.

[76] X. Li, "Scalable video compression via overcomplete motion compensated wavelet coding," *Signal Processing: Image Communication*, vol. 19, no. 7, pp. 637–651, 2004.

[77] Y. Andreopoulos, A. Munteanu, G. van der Auwera, P. Schelkens, and J. Cornelis, "Scalable wavelet video-coding with in-band prediction—implementation and experimental results," in *Proceedings of IEEE International Conference on Image Processing (ICIP '02)*, vol. 3, pp. 729–732, Rochester, NY, USA, September 2002.

[78] Y. Andreopoulos, A. Munteanu, G. Van der Auwera, P. Schelkens, and J. Cornelis, "A new method for complete-to-overcomplete discrete wavelet transforms," in *Proceedings of the 14th International Conference on Digital Signal Processing (DSP '02)*, vol. 2, pp. 501–504, Santorini, Greece, July 2002.

[79] Y. Andreopoulos, A. Munteanu, G. Van der Auwera, J. P. H. Cornelis, and P. Schelkens, "Complete-to-overcomplete discrete wavelet transforms: theory and applications," *IEEE Transactions on Signal Processing*, vol. 53, no. 4, pp. 1398–1412, 2005.

[80] X. Li, "New results of phase shifting in the wavelet space," *IEEE Signal Processing Letters*, vol. 10, no. 7, pp. 193–195, 2003.

[81] S. Cui, Y. Wang, and J. E. Fowler, "Mesh-based motion estimation and compensation in the wavelet domain using a redundant transform," in *Proceedings of IEEE International Conference on Image Processing (ICIP '02)*, vol. 1, pp. 693–696, Rochester, NY, USA, September 2002.

[82] S. Cui, Y. Wang, and J. E. Fowler, "Motion estimation and compensation in the redundant-wavelet domain using triangle meshes," *Signal Processing: Image Communication*, vol. 21, no. 7, pp. 586–598, 2006.

[83] S. Cui, Y. Wang, and J. E. Fowler, "Multihypothesis motion compensation in the redundant wavelet domain," in *Proceedings of IEEE International Conference on Image Processing (ICIP '03)*, vol. 2, pp. 53–56, Barcelona, Spain, September 2003.

[84] J. E. Fowler, S. Cui, and Y. Wang, "Motion compensation via redundant-wavelet multihypothesis," *IEEE Transactions on Image Processing*, vol. 15, no. 10, pp. 3102–3113, 2006.

[85] A. Secker and D. Taubman, "Highly scalable video compression using a lifting-based 3D wavelet transform with deformable mesh motion compensation," in *Proceedings of IEEE International Conference on Image Processing (ICIP '02)*, vol. 3, pp. 749–752, Rochester, NY, USA, September 2002.

[86] D. Taubman, "Successive refinement of video: fundamental issues, past efforts and new directions," in *Visual Communications and Image Processing*, T. Ebrahimi and T. Sikora, Eds., vol. 5150 of *Proceedings of SPIE*, pp. 649–663, Lugano, Switzerland, July 2003.

[87] J.-R. Ohm, "Advances in scalable video coding," *Proceedings of the IEEE*, vol. 93, no. 1, pp. 42–56, 2005.

[88] J.-R. Ohm, "Three-dimensional subband coding with motion compensation," *IEEE Transactions on Image Processing*, vol. 3, no. 5, pp. 559–571, 1994.

[89] S.-J. Choi and J. W. Woods, "Motion-compensated 3-D subband coding of video," *IEEE Transactions on Image Processing*, vol. 8, no. 2, pp. 155–167, 1999.

[90] B. Pesquet-Popescu and V. Bottreau, "Three-dimensional lifting schemes for motion compensated video compression," in *Proceedings of IEEE International Conference on Acoustics, Speech, and Signal Processing (ICASSP '01)*, vol. 3, pp. 1793–1796, Salt Lake City, Utah, USA, May 2001.

[91] A. Secker and D. Taubman, "Motion-compensated highly scalable video compression using an adaptive 3D wavelet transform based on lifting," in *Proceedings of IEEE International Conference on Image Processing (ICIP '01)*, vol. 2, pp. 1029–1032, Thessaloniki, Greece, October 2001.

[92] A. Golwelkar and J. W. Woods, "Scalable video compression using longer motion compensated temporal filters," in *Visual Communications and Image Processing*, T. Ebrahimi and T. Sikora, Eds., vol. 5150 of *Proceedings of SPIE*, pp. 1406–1416, Lugano, Switzerland, July 2003.

[93] M. Flierl and B. Girod, "Video coding with motion-compensated lifted wavelet transforms," *Signal Processing: Image Communication*, vol. 19, no. 7, pp. 561–575, 2004.

[94] V. Bottreau, M. Bénetière, B. Felts, and B. Pesquet-Popescu, "A fully scalable 3D subband video codec," in *Proceedings of IEEE International Conference on Image Processing (ICIP '01)*, vol. 2, pp. 1017–1020, Thessaloniki, Greece, October 2001.

[95] A. Secker and D. Taubman, "Lifting-based invertible motion adaptive transform (LIMAT) framework for highly scalable video compression," *IEEE Transactions on Image Processing*, vol. 12, no. 12, pp. 1530–1542, 2003.

[96] L. Luo, F. Wu, S. Li, Z. Xiong, and Z. Zhuang, "Advanced motion threading for 3D wavelet video coding," *Signal Processing: Image Communication*, vol. 19, no. 7, pp. 601–616, 2004.

[97] D. S. Turaga and M. van der Schaar, "Wavelet coding for video streaming using new unconstrained motion

compensated temporal filtering," in *Proceedings of International Thyrrhenian Workshop on Digital Communications (IWDC '02)*, pp. 41–48, Capri, Italy, September 2002, Advanced Methods for Multimedia Signal Processing.

[98] D. S. Turaga, M. van der Schaar, Y. Andreopoulos, A. Munteanu, and P. Schelkens, "Unconstrained motion compensated temporal filtering (UMCTF) for efficient and flexible interframe wavelet video coding," *Signal Processing: Image Communication*, vol. 20, no. 1, pp. 1–19, 2005.

[99] Y. Andreopoulos, A. Munteanu, J. Barbarien, M. van der Schaar, J. Cornelis, and P. Schelkens, "In-band motion compensated temporal filtering," *Signal Processing: Image Communication*, vol. 19, no. 7, pp. 653–673, 2004.

[100] Y. Wang, S. Cui, and J. E. Fowler, "3D video coding using redundant-wavelet multihypothesis and motion-compensated temporal filtering," in *Proceedings of IEEE International Conference on Image Processing (ICIP '03)*, vol. 2, pp. 755–758, Barcelona, Spain, September 2003.

[101] Y. Wang, S. Cui, and J. E. Fowler, "3D video coding with redundant-wavelet multihypothesis," *IEEE Transactions on Circuits and Systems for Video Technology*, vol. 16, no. 2, pp. 166–177, 2006.

[102] C. Tillier and B. Pesquet-Popescu, "3D, 3-band, 3-tap temporal lifting for scalable video coding," in *Proceedings of IEEE International Conference on Image Processing (ICIP '03)*, vol. 2, pp. 779–782, Barcelona, Spain, September 2003.

[103] C. Tillier, B. Pesquet-Popescu, and M. van der Schaar, "3-band motion-compensated temporal structures for scalable video coding," *IEEE Transactions on Image Processing*, vol. 15, no. 9, pp. 2545–2557, 2006.

[104] M. Trocan, C. Tillier, B. Pesquet-Popescu, and M. van der Schaar, "A 5-band temporal lifting scheme for video surveillance," in *Proceedings of the 8th IEEE Workshop on Multimedia Signal Processing (MMSP '06)*, pp. 278–281, Victoria, BC, Canada, October 2006.

[105] G. Pau, C. Tillier, B. Pesquet-Popescu, and H. Heijmans, "Motion compensation and scalability in lifting-based video coding," *Signal Processing: Image Communication*, vol. 19, no. 7, pp. 577–600, 2004.

[106] P. Chen, K. Hanke, T. Rusert, and J. W. Woods, "Improvements to the MC-EZBC scalable video coder," in *Proceedings of IEEE International Conference on Image Processing (ICIP '03)*, vol. 2, pp. 81–84, Barcelona, Spain, September 2003.

[107] Y. Wu and J. W. Woods, "Directional spatial I-blocks for the MC-EZBC video coder," in *Proceedings of IEEE International Conference on Acoustics, Speech, and Signal Processing (ICASSP '04)*, vol. 3, pp. 129–132, Montreal, Canada, May 2004.

[108] J. W. Woods and G. Lilienfield, "A resolution and frame-rate scalable subband/wavelet video coder," *IEEE Transactions on Circuits and Systems for Video Technology*, vol. 11, no. 9, pp. 1035–1044, 2001.

[109] J. C. Ye and M. van der Schaar, "Fully scalable 3-D overcomplete wavelet video coding using adaptive motion compensated temporal filtering," in *Visual Communications and Image Processing*, T. Ebrahimi and T. Sikora, Eds., vol. 5150 of *Proceedings of SPIE*, pp. 1169–1180, Lugano, Switzerland, July 2003.

[110] Y. Andreopoulos, M. van der Schaar, A. Munteanu, J. Barbarien, P. Schelkens, and J. Cornelis, "Complete-to-overcomplete discrete wavelet transforms for scalable video coding with MCTF," in *Visual Communications and Image Processing*, T. Ebrahimi and T. Sikora, Eds., vol. 5150 of *Proceedings of SPIE*, pp. 719–731, Lugano, Switzerland, July 2003.

[111] V. Seran and L. P. Kondi, "3D based video coding in the overcomplete discrete wavelet transform domain with reduced delay requirements," in *Proceedings of IEEE International Conference on Image Processing (ICIP '05)*, vol. 3, pp. 233–236, Genova, Italy, September 2005.

[112] N. Mehrseresht and D. Taubman, "A flexible structure for fully scalable motion-compensated 3-D DWT with emphasis on the impact of spatial scalability," *IEEE Transactions on Image Processing*, vol. 15, no. 3, pp. 740–753, 2006.

[113] N. Mehrseresht and D. Taubman, "An efficient content-adaptive motion-compensated 3-D DWT with enhanced spatial and temporal scalability," *IEEE Transactions on Image Processing*, vol. 15, no. 6, pp. 1397–1412, 2006.

[114] H. Schwarz, D. Marpe, and T. Wiegand, "Overview of the scalable H.264/MPEG4-AVC extension," in *Proceedings of IEEE International Conference on Image Processing (ICIP '06)*, pp. 161–164, Atlanta, Ga, USA, October 2006.

[115] H. Schwarz, D. Marpe, and T. Wiegand, "Overview of the scalable video coding standard," to appear in *IEEE Transactions on Circuits and Systems for Video Technology*.

[116] *Information Technology—JPEG 2000 Image Coding System—Part 3: Motion JPEG 2000*, ISO/IEC 15444-3, 2003.

[117] T. André, M. Cagnazzo, M. Antonini, and M. Barlaud, "JPEG2000-compatible scalable scheme for wavelet-based video coding," *EURASIP Journal on Image and Video Processing*, vol. 2007, Article ID 30852, 11 pages, 2007.

[118] G. Karlsson and M. Vetterli, "Three dimensional sub-band coding of video," in *Proceedings of IEEE International Conference on Acoustics, Speech, and Signal Processing (ICASSP '88)*, vol. 2, pp. 1100–1103, New York, NY, USA, April 1988.

[119] N. Kingsbury, "Complex wavelets for shift invariant analysis and filtering of signals," *Applied and Computational Harmonic Analysis*, vol. 10, no. 3, pp. 234–253, 2001.

[120] T. H. Reeves and N. Kingsbury, "Overcomplete image coding using iterative projection-based noise shaping," in *Proceedings of IEEE International Conference on Image Processing (ICIP '02)*, vol. 3, pp. 597–600, Rochester, NY, USA, September 2002.

[121] I. W. Selesnick and K. Y. Li, "Video denoising using 2D and 3D dual-tree complex wavelet transforms," in *Wavelets: Applications in Signal and Image Processing X*, vol. 5207 of *Proceedings of SPIE*, pp. 607–618, San Diego, Calif, USA, August 2003.

[122] B. Wang, Y. Wang, I. Selesnick, and A. Vetro, "An investigation of 3D dual-tree wavelet transform for video coding," in *Proceedings of IEEE International Conference on Image Processing (ICIP '04)*, vol. 2, pp. 1317–1320, Singapore, October 2004.

[123] W. Sweldens, "Lifting scheme: a new philosophy in biorthogonal wavelet constructions," in *Wavelet Applications in Signal and Image Processing III*, A. F. Laine, M. A. Unser, and M. V. Wickerhauser, Eds., vol. 2569 of *Proceedings of SPIE*, pp. 68–79, San Diego, Calif, USA, July 1995.

[124] J. B. Boettcher and J. E. Fowler, "Video coding using a complex wavelet transform and set partitioning," *IEEE Signal Processing Letters*, vol. 14, no. 9, 2007.

[125] P. Desarte, B. Macq, and D. T. M. Slock, "Signal-adapted multiresolution transform for image coding," *IEEE Transactions on Information Theory*, vol. 38, no. 2, part 2, pp. 897–904, 1992.

[126] A. Uhl, "Image compression using non-stationary and inhomogeneous multiresolution analyses," *Image and Vision Computing*, vol. 14, no. 5, pp. 365–371, 1996.

[127] W. Sweldens, "The lifting scheme: a construction of second generation wavelets," *SIAM Journal on Mathematical Analysis*, vol. 29, no. 2, pp. 511–546, 1998.

[128] I. Daubechies and W. Sweldens, "Factoring wavelet transforms into lifting steps," *Journal of Fourier Analysis and Applications*, vol. 4, no. 3, pp. 247–269, 1998.

[129] W. Sweldens and P. Schröder, "Building your own wavelets at home," in *Wavelets in Computer Graphics*, ACM SIGGRAPH Course Notes, pp. 15–87, ACM Press, New York, NY, USA, 1996.

[130] R. Claypoole, G. Davis, W. Sweldens, and R. Baraniuk, "Nonlinear wavelet transforms for image coding," in *Proceedings of the 31st Asilomar Conference on Signals, Systems & Computers*, vol. 1, pp. 662–667, Pacific Grove, Calif, USA, November 1997.

[131] R. L. Claypoole Jr., G. M. Davis, W. Sweldens, and R. G. Baraniuk, "Nonlinear wavelet transforms for image coding via lifting," *IEEE Transactions on Image Processing*, vol. 12, no. 12, pp. 1449–1459, 2003.

[132] N. V. Boulgouris and M. G. Strintzis, "Reversible multiresolution image coding based on adaptive lifting," in *Proceedings of IEEE International Conference on Image Processing (ICIP '99)*, vol. 3, pp. 546–550, Kobe, Japan, October 1999.

[133] N. V. Boulgouris, D. Tzovaras, and M. G. Strintzis, "Lossless image compression based on optimal prediction, adaptive lifting, and conditional arithmetic coding," *IEEE Transactions on Image Processing*, vol. 10, no. 1, pp. 1–14, 2001.

[134] D. Taubman, "Adaptive, non-separable lifting transforms for image compression," in *Proceedings of IEEE International Conference on Image Processing (ICIP '99)*, vol. 3, pp. 772–776, Kobe, Japan, October 1999.

[135] Ö. N. Gerek and A. E. Çetin, "Adaptive polyphase subband decomposition structures for image compression," *IEEE Transactions on Image Processing*, vol. 9, no. 10, pp. 1649–1660, 2000.

[136] Ö. N. Gerek and A. E. Çetin, "A 2-D orientation-adaptive prediction filter in lifting structures for image coding," *IEEE Transactions on Image Processing*, vol. 15, no. 1, pp. 106–111, 2006.

[137] G. Piella and H. J. A. M. Heijmans, "An adaptive update lifting scheme with perfect reconstruction," in *Proceedings of IEEE International Conference on Image Processing (ICIP '01)*, vol. 3, pp. 190–193, Thessaloniki, Greece, October 2001.

[138] H. J. A. M. Heijmans, G. Piella, and B. Pesquet-Popescu, "Building adaptive 2D wavelet decompositions by update lifting," in *Proceedings of IEEE International Conference on Image Processing (ICIP '02)*, vol. 1, pp. 397–400, Rochester, NY, USA, September 2002.

[139] G. Piella and H. J. A. M. Heijmans, "Adaptive lifting schemes with perfect reconstruction," *IEEE Transactions on Signal Processing*, vol. 50, no. 7, pp. 1620–1630, 2002.

[140] B. Pesquet-Popescu, G. Piella, and H. J. A. M. Heijmans, "Adaptive update lifting with gradient criteria modeling high-order differences," in *Proceedings of IEEE International Conference on Acoustics, Speech, and Signal Processing (ICASSP '02)*, vol. 2, pp. 1417–1420, Orlando, Fla, USA, May 2002.

[141] G. Piella, B. Pesquet-Popescu, and H. J. A. M. Heijmans, "Adaptive update lifting with a decision rule based on derivative filters," *IEEE Signal Processing Letters*, vol. 9, no. 10, pp. 329–332, 2002.

[142] B. Pesquet-Popescu, H. J. A. M. Heijmans, G. C. K. Abhayaratne, and G. Piella, "Quantization of adaptive 2D wavelet decompositions," in *Proceedings of IEEE International Conference on Image Processing (ICIP '03)*, vol. 3, pp. 209–212, Barcelona, Spain, September 2003.

[143] G. Piella, B. Pesquet-Popescu, and H. J. A. M. Heijmans, "Gradient-driven update lifting for adaptive wavelets," *Signal Processing: Image Communication*, vol. 20, no. 9-10, pp. 813–831, 2005.

[144] G. Piella, B. Pesquet-Popescu, H. J. A. M. Heijmans, and G. Pau, "Combining seminorms in adaptive lifting schemes and applications to image analysis and compression," *Journal of Mathematical Imaging and Vision*, vol. 25, no. 2, pp. 203–226, 2006.

[145] H. J. A. M. Heijmans, G. Piella, and B. Pesquet-Popescu, "Adaptive wavelets for image compression using update lifting: quantization and error analysis," *International Journal of Wavelets, Multiresolution and Information Processing*, vol. 4, no. 1, pp. 41–63, 2006.

[146] J. Hattay, A. Benazza-Benyahia, and J.-C. Pesquet, "Adaptive lifting for multicomponent image coding through quadtree partitioning," in *Proceedings of IEEE International Conference on Acoustics, Speech, and Signal Processing (ICASSP '05)*, vol. 2, pp. 213–216, Philadelphia, Pa, USA, March 2005.

[147] A. Gouze, M. Antonini, and M. Barlaud, "Quincunx lifting scheme for lossy image compression," in *Proceedings of IEEE International Conference on Image Processing (ICIP '00)*, vol. 1, pp. 665–668, Vancouver, BC, Canada, September 2000.

[148] A. Gouze, M. Antonini, M. Barlaud, and B. Macq, "Optimized lifting scheme for two-dimensional quincunx sampling images," in *Proceedings of IEEE International Conference on Image Processing (ICIP '01)*, vol. 2, pp. 253–256, Thessaloniki, Greece, October 2001.

[149] A. Gouze, M. Antonini, M. Barlaud, and B. Macq, "Design of signal-adapted multidimensional lifting scheme for lossy coding," *IEEE Transactions on Image Processing*, vol. 13, no. 12, pp. 1589–1603, 2004.

[150] J. Solé and P. Salembier, "Quadratic interpolation and linear lifting design," *EURASIP Journal on Image and Video Processing*, vol. 2007, Article ID 37843, 11 pages, 2007.

[151] D. D. Muresan and T. W. Parks, "Adaptively quadratic (AQua) image interpolation," *IEEE Transactions on Image Processing*, vol. 13, no. 5, pp. 690–698, 2004.

[152] Y. Zhu, S. C. Schwartz, and M. T. Orchard, "Wavelet domain image interpolation via statistical estimation," in *Proceedings of IEEE International Conference on Image Processing (ICIP '01)*, vol. 3, pp. 840–843, Thessaloniki, Greece, October 2001.

[153] S. G. Chang, G. Cvetković, and M. Vetterli, "Resolution enhancement of images using wavelet transform extrema extrapolation," in *Proceedings of IEEE International Conference on Acoustics, Speech, and Signal Processing (ICASSP '95)*, vol. 4, pp. 2379–2382, Detroit, Mich, USA, May 1995.

[154] S. G. Chang, Z. Cvetković, and M. Vetterli, "Locally adaptive wavelet-based image interpolation," *IEEE Transactions on Image Processing*, vol. 15, no. 6, pp. 1471–1485, 2006.

[155] W. K. Carey, D. B. Chuang, and S. S. Hemami, "Regularity-preserving image interpolation," *IEEE Transactions on Image Processing*, vol. 8, no. 9, pp. 1293–1297, 1999.

[156] S. Mallat and S. Zhong, "Characterization of signals from multiscale edges," *IEEE Transactions on Pattern Analysis and Machine Intelligence*, vol. 14, no. 7, pp. 710–732, 1992.

[157] P. L. Combettes, "The foundations of set theoretic estimation," *Proceedings of the IEEE*, vol. 81, no. 2, pp. 182–208, 1993.

[158] D. D. Muresan and T. W. Parks, "Prediction of image detail," in *Proceedings of IEEE International Conference on Image Processing (ICIP '00)*, vol. 2, pp. 323–326, Vancouver, BC, Canada, September 2000.

[159] K. Kinebuchi, D. D. Muresan, and T. W. Parks, "Image interpolation using wavelet-based hidden Markov trees," in *Proceedings of IEEE International Conference on Acoustics, Speech, and Signal Processing (ICASSP '01)*, vol. 3, pp. 1957–1960, Salt Lake, Utah, USA, May 2001.

[160] D. H. Woo, I. K. Eom, and Y. S. Kim, "Image interpolation based on inter-scale dependency in wavelet domain," in *Proceedings of IEEE International Conference on Image Processing (ICIP '04)*, vol. 3, pp. 1687–1690, Singapore, October 2004.

[161] V. K. Goyal, "Multiple description coding: compression meets the network," *IEEE Signal Processing Magazine*, vol. 18, no. 5, pp. 74–93, 2001.

[162] L. Ozarow, "On a source-coding problem with two channels and three receivers," *Bell System Technical Journal*, vol. 59, no. 10, pp. 1909–1921, 1980.

[163] A. E. Gamal and T. Cover, "Achievable rates for multiple descriptions," *IEEE Transactions on Information Theory*, vol. 28, no. 6, pp. 851–857, 1982.

[164] R. Venkataramani, G. Kramer, and V. K. Goyal, "Multiple description coding with many channels," *IEEE Transactions on Information Theory*, vol. 49, no. 9, pp. 2106–2114, 2003.

[165] J. G. Apostolopoulos, "Reliable video communication over lossy packet networks using multiple state encoding and path diversity," in *Visual Communications and Image Processing*, B. Girod, C. A. Bouman, and E. G. Steinbach, Eds., vol. 4310 of *Proceedings of SPIE*, pp. 392–409, San Jose, Calif, USA, January 2001.

[166] V. A. Vaishampayan, "Design of multiple description scalar quantizers," *IEEE Transactions on Information Theory*, vol. 39, no. 3, pp. 821–834, 1993.

[167] V. A. Vaishampayan and J. Domaszewicz, "Design of entropy-constrained multiple-description scalar quantizers," *IEEE Transactions on Information Theory*, vol. 40, no. 1, pp. 245–250, 1994.

[168] S. D. Servetto, K. Ramchandran, V. A. Vaishampayan, and K. Nahrstedt, "Multiple description wavelet based image coding," *IEEE Transactions on Image Processing*, vol. 9, no. 5, pp. 813–826, 2000.

[169] W. Jiang and A. Ortega, "Multiple description coding via polyphase transform and selective quantization," in *Visual Communications and Image Processing*, K. Aizawa, R. L. Stevenson, and Y.-Q. Zhang, Eds., vol. 3653 of *Proceedings of SPIE*, pp. 998–1008, San Jose, Calif, USA, January 1999.

[170] A. C. Miguel, A. E. Mohr, and E. A. Riskin, "SPIHT for generalized multiple description coding," in *Proceedings of IEEE International Conference on Image Processing (ICIP '99)*, vol. 3, pp. 842–846, Kobe, Japan, October 1999.

[171] Y. Wang, M. T. Orchard, and A. R. Reibman, "Multiple description image coding for noisy channels by pairing transform coefficients," in *Proceedings of the 1st IEEE Workshop on Multimedia Signal Processing*, pp. 419–424, Princeton, NJ, USA, June 1997.

[172] Y. Wang, M. T. Orchard, and A. R. Reibman, "Optimal pairwise correlating transforms for multiple description coding," in *Proceedings of IEEE International Conference on Image Processing (ICIP '98)*, vol. 1, pp. 679–683, Chicago, Ill, USA, October 1998.

[173] Y. Wang, M. T. Orchard, V. Vaishampayan, and A. R. Reibman, "Multiple description coding using pairwise correlating transforms," *IEEE Transactions on Image Processing*, vol. 10, no. 3, pp. 351–366, 2001.

[174] V. K. Goyal and J. Kovačević, "Optimal multiple description transform coding of Gaussian vectors," in *Proceedings of IEEE Data Compression Conference (DCC '98)*, J. A. Storer and M. Cohn, Eds., pp. 388–397, Snowbird, Utah, USA, March-April 1998.

[175] V. K. Goyal and J. Kovačević, "Generalized multiple description coding with correlating transforms," *IEEE Transactions on Information Theory*, vol. 47, no. 6, pp. 2199–2224, 2001.

[176] X. Yang and K. Ramchandran, "Optimal multiple description subband coding," in *Proceedings of IEEE International Conference on Image Processing (ICIP '98)*, vol. 1, pp. 654–658, Chicago, Ill, USA, October 1998.

[177] X. Yang and K. Ramchandran, "Optimal subband filter banks for multiple description coding," *IEEE Transactions on Information Theory*, vol. 46, no. 7, pp. 2477–2490, 2000.

[178] V. K. Goyal, J. Kovačević, and M. Vetterli, "Quantized frame expansions as source-channel codes for erasure channels," in *Proceedings of IEEE Data Compression Conference (DCC '99)*, J. A. Storer and M. Cohn, Eds., pp. 326–335, Snowbird, Utah, USA, March 1999.

[179] V. K. Goyal, J. Kovačević, and J. A. Kelner, "Quantized frame expansions with erasures," *Applied and Computational Harmonic Analysis*, vol. 10, no. 3, pp. 203–233, 2001.

[180] J. Kovačević, P. L. Dragotti, and V. K. Goyal, "Filter bank frame expansions with erasures," *IEEE Transactions on Information Theory*, vol. 48, no. 6, pp. 1439–1450, 2002.

[181] S. D. Servetto, V. A. Vaishampayan, and N. J. A. Sloane, "Multiple description lattice vector quantization," in *Proceedings of IEEE Data Compression Conference (DCC '99)*, J. A. Storer and M. Cohn, Eds., pp. 13–22, Snowbird, Utah, USA, March 1999.

[182] V. A. Vaishampayan, N. J. A. Sloane, and S. D. Servetto, "Multiple-description vector quantization with lattice codebooks: design and analysis," *IEEE Transactions on Information Theory*, vol. 47, no. 5, pp. 1718–1734, 2001.

[183] J. A. Kelner, V. K. Goyal, and J. Kovačević, "Multiple description lattice vector quantization: variations and extensions," in *Proceedings of IEEE Data Compression Conference (DCC '00)*, J. A. Storer and M. Cohn, Eds., pp. 480–489, Snowbird, Utah, USA, March 2000.

[184] V. K. Goyal, J. A. Kelner, and J. Kovačević, "Multiple description vector quantization with a coarse lattice," *IEEE Transactions on Information Theory*, vol. 48, no. 3, pp. 781–788, 2002.

[185] T. Berger, *Rate Distortion Theory*, Prentice-Hall, Englewood Cliffs, NJ, USA, 1971.

[186] T. M. Cover and J. A. Thomas, *Elements of Information Theory*, John Wiley & Sons, Hoboken, NJ, USA, 2nd edition, 2006.

[187] S. S. Pradhan and K. Ramchandran, "On the optimality of block orthogonal transforms for multiple description coding of Gaussian vector sources," *IEEE Signal Processing Letters*, vol. 7, no. 4, pp. 76–78, 2000.

[188] V. K. Goyal, M. Vetterli, and N. T. Thao, "Quantized overcomplete expansions in $\mathbb{R}^N$: analysis, synthesis, and algorithms," *IEEE Transactions on Information Theory*, vol. 44, no. 1, pp. 16–31, 1998.

[189] W. S. Lee, M. R. Pickering, M. R. Frater, and J. F. Arnold, "A robust codec for transmission of very low bit-rate video over channels with bursty errors," *IEEE Transactions on Circuits*

and Systems for Video Technology, vol. 10, no. 8, pp. 1403–1412, 2000.

[190] A. R. Reibman, H. Jafarkhani, Y. Wang, M. T. Orchard, and R. Puri, "Multiple-description video coding using motion-compensated temporal prediction," *IEEE Transactions on Circuits and Systems for Video Technology*, vol. 12, no. 3, pp. 193–204, 2002.

[191] I. V. Bajic and J. W. Woods, "Domain-based multiple description coding of images and video," *IEEE Transactions on Image Processing*, vol. 12, no. 10, pp. 1211–1225, 2003.

[192] N. Franchi, M. Fumagalli, R. Lancini, and S. Tubaro, "Multiple description video coding for scalable and robust transmission over IP," *IEEE Transactions on Circuits and Systems for Video Technology*, vol. 15, no. 3, pp. 321–334, 2005.

[193] Y. Wang, A. R. Reibman, and S. Lin, "Multiple description coding for video delivery," *Proceedings of the IEEE*, vol. 93, no. 1, pp. 57–70, 2005.

[194] V. A. Vaishampayan and S. John, "Balanced interframe multiple description video compression," in *Proceedings of IEEE International Conference on Image Processing (ICIP '99)*, vol. 3, pp. 812–816, Kobe, Japan, October 1999.

[195] Y. Wang and S. Lin, "Error-resilient video coding using multiple description motion compensation," *IEEE Transactions on Circuits and Systems for Video Technology*, vol. 12, no. 6, pp. 438–452, 2002.

[196] M. van der Schaar and D. S. Turaga, "Multiple description scalable coding using wavelet-based motion compensated temporal filtering," in *Proceedings of IEEE International Conference on Image Processing (ICIP '03)*, vol. 3, pp. 489–492, Barcelona, Spain, September 2003.

[197] C. Tillier, B. Pesquet-Popescu, and M. van der Schaar, "Multiple descriptions scalable video coding," in *Proceedings of the 12th European Signal Processing Conference (EUSIPCO '04)*, Vienna, Austria, September 2004.

[198] J. Kim, R. M. Mersereau, and Y. Altunbasak, "Network-adaptive video streaming using multiple description coding and path diversity," in *Proceedings of IEEE International Conference on Multimedia and Expo (ICME '03)*, vol. 2, pp. 653–656, Baltimore, Md, USA, July 2003.

[199] N. Franchi, M. Fumagalli, G. Gatti, and R. Lancini, "A novel error-resilience scheme for a 3-D multiple description video coder," in *Proceedings of the Picture Coding Symposium (PSC '04)*, pp. 373–376, San Francisco, Calif, USA, December 2004.

[200] S. Cho and W. A. Pearlman, "Error resilient compression and transmission of scalable video," in *Applications of Digital Image Processing XXIII*, A. G. Tescher, Ed., vol. 4115 of *Proceedings of SPIE*, pp. 396–405, San Diego, Calif, USA, July 2000.

[201] C. E. Shannon, "Coding theorems for a discrete source with a fidelity criterion," *IRE International Convention Record*, vol. 7, part 4, pp. 142–163, 1959.

[202] M. Srinivasan and R. Chellappa, "Adaptive source-channel subband video coding for wireless channels," *IEEE Journal on Selected Areas in Communications*, vol. 16, no. 9, pp. 1830–1839, 1998.

[203] J. Hagenauer, "Rate-compatible punctured convolutional codes (RCPC codes) and their applications," *IEEE Transactions on Communications*, vol. 36, no. 4, pp. 389–400, 1988.

[204] G. Cheung and A. Zakhor, "Joint source/channel coding of scalable video over noisy channels," in *Proceedings of IEEE International Conference on Image Processing (ICIP '96)*, vol. 3, pp. 767–770, Lausanne, Switzerland, September 1996.

[205] G. Cheung and A. Zakhor, "Bit allocation for joint source/channel coding of scalable video," *IEEE Transactions on Image Processing*, vol. 9, no. 3, pp. 340–356, 2000.

[206] Y. Shoham and A. Gersho, "Efficient bit allocation for an arbitrary set of quantizers," *IEEE Transactions on Acoustics, Speech, and Signal Processing*, vol. 36, no. 9, pp. 1445–1453, 1988.

[207] M. Bystrom and T. Stockhammer, "Dependent source and channel rate allocation for video transmission," *IEEE Transactions on Wireless Communications*, vol. 3, no. 1, pp. 258–268, 2004.

[208] J. Hagenauer and T. Stockhammer, "Channel coding and transmission aspects for wireless multimedia," *Proceedings of the IEEE*, vol. 87, no. 10, pp. 1764–1777, 1999.

[209] Z. Xiong, B.-J. Kim, and W. A. Pearlman, "Progressive video coding for noisy channels," in *Proceedings of IEEE International Conference on Image Processing (ICIP '98)*, vol. 1, pp. 334–337, Chicago, Ill, USA, October 1998.

[210] S. Cho and W. A. Pearlman, "A full-featured, error-resilient, scalable wavelet video codec based on the set partitioning in hierarchical trees (SPIHT) algorithm," *IEEE Transactions on Circuits and Systems for Video Technology*, vol. 12, no. 3, pp. 157–171, 2002.

[211] Z. Zhang, G. Liu, and Y. Yang, "Progressive source-channel coding of video for unknown noisy channels," in *Proceedings of IEEE International Conference on Acoustics, Speech, and Signal Processing (ICASSP '02)*, vol. 3, pp. 2493–2496, Orlando, Fla, USA, May 2002.

[212] R. G. Gallager, "Low-density parity-check codes," *IRE Transacations on Information Theory*, vol. 8, no. 1, pp. 21–28, 1962.

[213] D. J. C. MacKay, "Good error-correcting codes based on very sparse matrices," *IEEE Transactions on Information Theory*, vol. 45, no. 2, pp. 399–431, 1999.

[214] N. Farvardin and V. Vaishampayan, "Optimal quantizer design for noisy channels: an approach to combined source-channel coding," *IEEE Transactions on Information Theory*, vol. 33, no. 6, pp. 827–838, 1987.